Ryoji Kobayashi
Department of Pediatrics, Sapporo Hokuyu Hospital, Sapporo, Japan

Etsuro Ito
Department of Pediatrics, Hirosaki University School of Medicine, Hirosaki, Japan

Hiroshi Yagasaki
Department of Pediatrics, School of Medicine, Nihon University, Tokyo, Japan

Akira Ohara
Division of Blood Transfusion, Toho University Omori Hospital, Tokyo, Japan

Akira Kikuchi
Department of Pediatrics, Teikyo University School of Medicine, Tokyo, Japan

Akira Morimoto
Department of Pediatrics, Jichi Medical University School of Medicine, Tochigi, Japan

Hiromasa Yabe
Department of Cell Transplantation and Regenerative Medicine, Tokai University School of Medicine, Isehara, Japan

Kazuko Kudo
Division of Hematology and Oncology, Shizuoka Children's Hospital, Shizuoka, Japan

Ken-ichiro Watanabe
Department of Pediatrics, Graduate School of Medicine, Kyoto University, Kyoto, Japan

Shouichi Ohga
Department of Perinatal and Pediatric Medicine, Graduate School of Medical Sciences, Kyushu University, Fukuoka, Japan

Seiji Kojima
Department of Pediatrics, Nagoya Graduate School of Medicine, Nagoya, Japan

on behalf of the Japan Childhood Aplastic Anemia Study Group

Conflict-of-interest disclosure: The authors declare no competing financial interests.

Correspondence: Dr Seiji Kojima, Nagoya Graduate School of Medicine, Tsurumai-cho 65, Showa-ku, Nagoya, Ai, Japan 466-8550; e-mail: kojimas@med.nagoya-u.ac.jp.

References

1. Dufour C, Bacigalupo A, Oneto R, et al. Rabbit ATG for aplastic anaemia treatment: a backward step? *Lancet*. 2011;378(9806):1831-1833.
2. Marsh JC, Bacigalupo A, Schrezenmeier H, et al. Prospective study of rabbit antithymocyte globulin and cyclosporine for aplastic anemia from the EBMT Severe Aplastic Anaemia Working Party. *Blood*. 2012;119(23):5391-5396.
3. Scheinberg P, Nunez O, Weinstein B, et al. Horse versus rabbit antithymocyte globulin in acquired aplastic anemia. *N Engl J Med*. 2011;365(5):430-438.
4. Kojima S, Hibi S, Kosaka Y, et al. Immunosuppressive therapy using antithymocyte globulin, cyclosporine, and danazol with or without human granulocyte colony-stimulating factor in children with acquired aplastic anemia. *Blood*. 2000;96(6):2049-2054.
5. Kosaka Y, Yagasaki H, Sano K, et al. Prospective multicenter trial comparing repeated immunosuppressive therapy with stem-cell transplantation from an alternative donor as second-line treatment for children with severe and very severe aplastic anemia. *Blood*. 2008;111(3):1054-1059.

To the editor:

Peripheral blood stem cells versus bone marrow in pediatric unrelated donor stem cell transplantation

The relative benefits and risks of peripheral blood stem cells (PBSCs) versus bone marrow (BM) for allogeneic hematopoietic stem cell transplantation (SCT) are still a matter of highly controversial debates.[1-3] The first randomized study comparing the 2 stem cell sources in unrelated donor SCT recently documented comparable overall and event-free survival, but indicated a higher risk for chronic graft-versus-host disease (GVHD) with PBSCs.[4] Only a few pediatric patients were included in this study even though the long-term sequelae of chronic GVHD are of particular concern in this patient group.

We retrospectively compared the long-term outcome of contemporaneous unrelated donor SCT in 220 children transplanted with BM (n = 102) or PBSCs (n = 118) for hematologic malignancies and reported to the German/Austrian pediatric registry for SCT. All patients had received myeloablative conditioning followed by unmanipulated SCT from HLA-matched unrelated donors. The PBSC and BM groups were comparable with regard to patient and donor age, sex, cytomegalovirus (CMV) serostatus, disease status at transplantation, GVHD prophylaxis, growth factor use, and degree of HLA matching. The groups differed with regard to disease category with slightly more myelodysplastic syndrome patients ($P = .02$) and a higher CD34-cell dose ($P = .001$) in the PBSC group.

Neutrophil and platelet engraftment were achieved significantly faster after PBSC than BM transplantation (Figure 1A-B). In this entirely pediatric cohort, the incidence of clinically relevant grade II-IV acute GVHD (Figure 1C) did not differ. Most importantly, the incidence of chronic GVHD (PBSCs vs BM: 35% vs 33%, respectively; $P = .9$) and extensive chronic GVHD (Figure 1D) proved low and was virtually identical in the 2 groups. With a median follow-up time of 3 years, overall survival (PBSCs vs BM: 50% ± 5% vs 46% ± 6%, respectively; $P = .63$) and event-free survival (PBSCs vs BM: 45% ± 5% vs 44% ± 6%, respectively; $P = .59$) were comparable (Figure 1E-F). In multivariable analysis, taking into account all parameters with $P < .2$ in univariate analysis, the only significant independent risk factor for treatment failure was advanced disease status at the time of transplantation (relative risk = 2.4, 95% confidence interval, 1.5-3.8; $P = .001$). In contrast, stem cell source (PBSCs vs BM) had no effect (relative risk = 1.1, 95% confidence interval, 0.7-1.6; $P = .8$).

Our registry-based analysis provides evidence that in pediatric recipients of HLA-matched unrelated-donor transplantation with consistent antithymocyte globulin (ATG) use during conditioning, transplantation with PBSCs and BM results in comparable clinical outcomes without detectable differences in the risk of acute or, more importantly, chronic GVHD. Consistent with a recent study underscoring the role of ATG for the prevention of acute and chronic GVHD,[5] the use of ATG in 96% of our transplantation procedures compared with only 27% in the above-mentioned randomized study by Anasetti et al[4] might be one of the key factors responsible for the overall low and comparable incidence of

Brief Report

RED CELLS, IRON, AND ERYTHROPOIESIS

Variant ALDH2 is associated with accelerated progression of bone marrow failure in Japanese Fanconi anemia patients

Asuka Hira,[1] Hiromasa Yabe,[2] Kenichi Yoshida,[3] Yusuke Okuno,[3] Yuichi Shiraishi,[4] Kenichi Chiba,[4] Hiroko Tanaka,[5] Satoru Miyano,[4,5] Jun Nakamura,[6] Seiji Kojima,[7] Seishi Ogawa,[3,8] Keitaro Matsuo,[9] Minoru Takata,[1] and Miharu Yabe[2]

[1]Laboratory of DNA Damage Signaling, Department of Late Effects Studies, Radiation Biology Center, Kyoto University, Kyoto, Japan; [2]Department of Cell Transplantation and Regenerative Medicine, Tokai University School of Medicine, Isehara, Japan; [3]Cancer Genomics Project, Graduate School of Medicine, [4]Laboratory of DNA Information Analysis, and [5]Laboratory of Sequence Analysis, Human Genome Center, Institute of Medical Science, The University of Tokyo, Tokyo, Japan; [6]Department of Environmental Sciences and Engineering, University of North Carolina at Chapel Hill, Chapel Hill, NC; [7]Department of Pediatrics, Nagoya University Graduate School of Medicine, Nagoya, Japan; [8]Department of Pathology and Tumor Biology, Graduate School of Medicine, Kyoto University, Kyoto, Japan; and [9]Department of Preventive Medicine, Kyushu University Faculty of Medical Sciences, Fukuoka, Japan

Key Points

- We found the defective ALDH2 variant is associated with accelerated progression of BMF in Japanese FA patients.
- The data support the view that aldehydes are an important source of genotoxicity in the human hematopoietic system.

Fanconi anemia (FA) is a severe hereditary disorder with defective DNA damage response and repair. It is characterized by phenotypes including progressive bone marrow failure (BMF), developmental abnormalities, and increased occurrence of leukemia and cancer. Recent studies in mice have suggested that the FA proteins might counteract aldehyde-induced genotoxicity in hematopoietic stem cells. Nearly half of the Japanese population carries a dominant-negative allele (rs671) of the aldehyde-catalyzing enzyme *ALDH2* (acetaldehyde dehydrogenase 2), providing an opportunity to test this hypothesis in humans. We examined 64 Japanese FA patients, and found that the *ALDH2* variant is associated with accelerated progression of BMF, while birth weight or the number of physical abnormalities was not affected. Moreover, malformations at some specific anatomic locations were observed more frequently in *ALDH2*-deficient patients. Our current data indicate that the level of ALDH2 activity impacts pathogenesis in FA, suggesting the possibility of a novel therapeutic approach. (*Blood.* 2013;122(18):3206-3209)

Introduction

Fanconi anemia (FA) is a genomic instability disorder with phenotypes including progressive bone marrow failure (BMF), developmental abnormalities, and increased occurrence of leukemia and cancer.[1] To date, 16 genes have been implicated in FA, and their products form a common DNA repair network ("FA pathway").[2,3] Because FA cells are hypersensitive to DNA interstrand crosslinks (ICLs), the FA pathway has been considered to be involved in the repair of ICLs.[2,3] However, it remains unclear what type of endogenous DNA damage is repaired through the FA pathway. Recent studies have suggested that FA cells are also sensitive to aldehydes,[4] which may create DNA adducts including ICLs or DNA-protein crosslinks. Furthermore, double knockout mice deficient in *Fancd2* and *Aldh2*, but neither of the single mutant mice, display an accelerated development of leukemia and BMF.[5,6] On the other hand, Fanc-deficient mice in general do not fully recapitulate the human FA phenotype, including overt BMF.[7] Thus, the role of aldehydes in the pathogenesis of human FA is still uncertain.

ALDH2 deficiency resulting from a Glu504Lys substitution (rs671, hereinafter referred to as the A allele) is highly prevalent in East Asian populations. The A allele (Lys504) acts as a dominant negative, since the variant form can suppress the activity of the Glu504 form (G allele) in GA heterozygotes by the formation of heterotetramers.[8] Individuals with the A variant experience flushing when drinking alcohol, and have an elevated risk of esophageal cancer with habitual drinking.[9] Because the frequency of the A allele is close to 50% in the Japanese population at large, some Japanese FA patients are expected to be deficient in *ALDH2*. We thus set out to determine the *ALDH2* status in a collection of Japanese FA patients.

Study design

The onset of BMF was defined according to the criteria used in the International Fanconi Anemia Registry (IFAR) study.[10] Criteria for diagnosis of aplastic anemia and other conditions are described in supplemental Methods (available on the *Blood* Web site). We observed physical abnormalities characteristic of FA, including skin abnormalities (hyperpigmentation and café au lait spots), low birth weight, growth defects, and malformations affecting

Submitted June 13, 2013; accepted August 27, 2013. Prepublished online as *Blood* First Edition paper, September 13, 2013; DOI 10.1182/blood-2013-06-507962.

The online version of this article contains a data supplement.

The publication costs of this article were defrayed in part by page charge payment. Therefore, and solely to indicate this fact, this article is hereby marked "advertisement" in accordance with 18 USC section 1734.

Table 1. Summary of genotypes and clinical characteristics of the patients studied

	Total	ALDH2 genotype		
		GG	GA	AA
No. of cases	64	36	25	3
Mutated FA gene*				
FANCA	39	26†	11	2
FANCG	15	7	8	—
FANCI	2	—	2	—
FANCM	1	—	1	—
FANCP	2	—	1	1
Unknown	5	3	2	—
Disease				
Aplastic anemia	2	2	—	—
Severe aplastic anemia	40	21	19	—
MDS/AML	22	13	6	3‡
Tongue cancer	2	1	1	—
Median months of onset (range)				
BMF	52 (0-297)	72 (27-297)	28 (7-87)	0 (0-7)
MDS/AML	118 (4-384)	156 (61-384)	85 (41-192)	4 (4-12)
No. of cases with SCT (%)	58 (91)	33 (92)	23 (92)	2 (67)
Median months at SCT (range)	118 (12-448)	130 (52-448)	86 (28-248)	25 (13-36)

–, no case was found.

*Mutations found in the patients were listed in supplemental Table 1. Some of them were presumptive because their functional significance has not been determined.

†Somatic mosaicism due to reversion was confirmed in 2 cases and suspected in 1 case.

‡In these cases, onset of severe aplastic anemia and MDS was essentially simultaneous.

skeletal systems and deep organs. Extensive malformation was defined as the involvement of at least 3 sites including at least 1 deep organ.[11] Mutation analysis of *FANCA/FANCC/FANCG* genes,[12] *ALDH2* genotyping,[13] multiplex ligation-mediated probe amplification (MLPA) test for *FANCA* (Falco), and whole-exome sequencing (WES)[14] were done as previously described. Details are provided as supplemental Methods. Development of BMF or acute myeloid leukemia (AML)/myelodysplasia (MDS) was analyzed by the Kaplan-Meier method or the cumulative incidence method,[15,16] respectively, since competing events (eg, death and stem cell transplantation [SCT]) existed in AML/MDS but not in BMF. This study was approved by the Research Ethics Committee of the Tokai University Hospital and Kyoto University. We obtained family informed consent from all subjects involved in this work in accordance with the Declaration of Helsinki.

Results and discussion

All of the patients in this study (n = 64; supplemental Table 1) were referred to the Tokai University Hospital because of pancytopenia, in some cases with MDS or leukemia. The clinical diagnosis of FA was made based on clinical presentation and diepoxybutane (DEB)-induced chromosome fragility tests in peripheral blood lymphocytes,[17] except for 3 cases in which the DEB test was negative due to *FANCA* reversion mosaicism (supplemental Tables 1-2). Most of the patients underwent allogeneic SCT, indicating that our patients probably represent an FA population with relatively severe hematologic symptoms.

To determine which FA gene was mutated in each of these patients, we applied combinations of polymerase chain reaction–based methods (n = 26), the MLPA test for *FANCA* mutations (n = 44), and WES (n = 29). In our WES analysis, >90% of the 50-Mb target sequences were analyzed by >10 independent reads (data not shown). Fifty-nine patients were found to have a mutation in FA genes in at least 1 allele, but 5 of them were mutation-free in the known 16 FA genes, even after WES (Table 1; supplemental Table 1). These unclassified cases might be caused by large deletions or intronic mutations that are difficult to detect with these methods,[18] or possibly mutations in a novel FA gene.

We determined the *ALDH2* genotype in our series of 64 patients (Table 1; supplemental Table 1). The distribution of the *ALDH2* variant alleles appeared not significantly different from the reported allele frequencies in the healthy Japanese population.[13] The occurrence of leukemia and/or MDS was also not significantly different between patients with GA and GG genotypes. Strikingly, however, we found that progression of BMF was accelerated in heterozygous carriers of the variant A allele compared with homozygous GG patients (Figure 1A-B). Moreover, the 3 individuals carrying AA alleles developed MDS with BMF at a very young age (Figure 1A-B). None of these 3 patients belonged to FA-D1 or FA-N, the FA subgroups with severe symptoms.[19,20] Patient number 3 had biallelic frameshift mutations (S115AfsX11) in *FANCP/SLX4*. By contrast, of the FA-P patients that have previously been reported, none have displayed particularly severe symptoms.[21-23]

FA is a heterogeneous disorder, and our cohort of patients is quite heterogeneous in terms of complementation groups and types of mutations (Table 1). To reduce some of the variability, we selected only the *FANCA* patients having nonsense, frameshift, or large deletion mutations identified at both alleles, (n = 12; supplemental Table 1), and repeated the analysis. A patient with probable *FANCA* reversion (patient number 55) was excluded. In this subset of patients, a highly significant statistical difference was reproduced in BMF progression (Figure 1C) but not in AML/MDS development (data not shown).

We could not detect any significant difference in terms of the percentage of birth weight (Figure 1D) or number of physical abnormalities (Figure 1E) that correlated with the *ALDH2* genotypes. However, a significant difference was observed in the incidence of each class of malformations in the case of radial, cardiovascular, skeletal, or kidney anomalies, and in the incidence of extensive malformation (Figure 1F).

In conclusion, our current data indicate that endogenous aldehydes are an important source of genotoxicity in the human hematopoietic system, and the FA pathway counteracts them. If the FA pathway is compromised, hematopoietic stem cells (HSCs) likely accumulate aldehyde-induced DNA damage, resulting in BMF due to p53/p21-mediated cell death or senescence.[6,24] Consistent with this model, a recent study showed that the HSCs in *aldh2/fancd2* double knockout mice accumulate more DNA damage than HSCs in either of the single knockout mice.[6] Because some *ALDH2*-proficient FA patients developed BMF early, other modifier genes or environmental factors might affect levels of aldehydes or other genotoxic substances. Interestingly, our data predict that Japanese FA patients in general develop BMF at an earlier age compared with patients of other ethnic origins. We need to establish a Japanese FA registry similar to IFAR to test whether this is true or not. Finally, it seems worth considering *ALDH2* agonists such as Alda-1 as protective drugs against BMF in FA patients. Alda-1 can stimulate the enzymatic activity of both the normal and variant ALDH2,[25] suggesting that Alda-1 or a similar drug could be beneficial even for *ALDH2*-proficient FA cases.

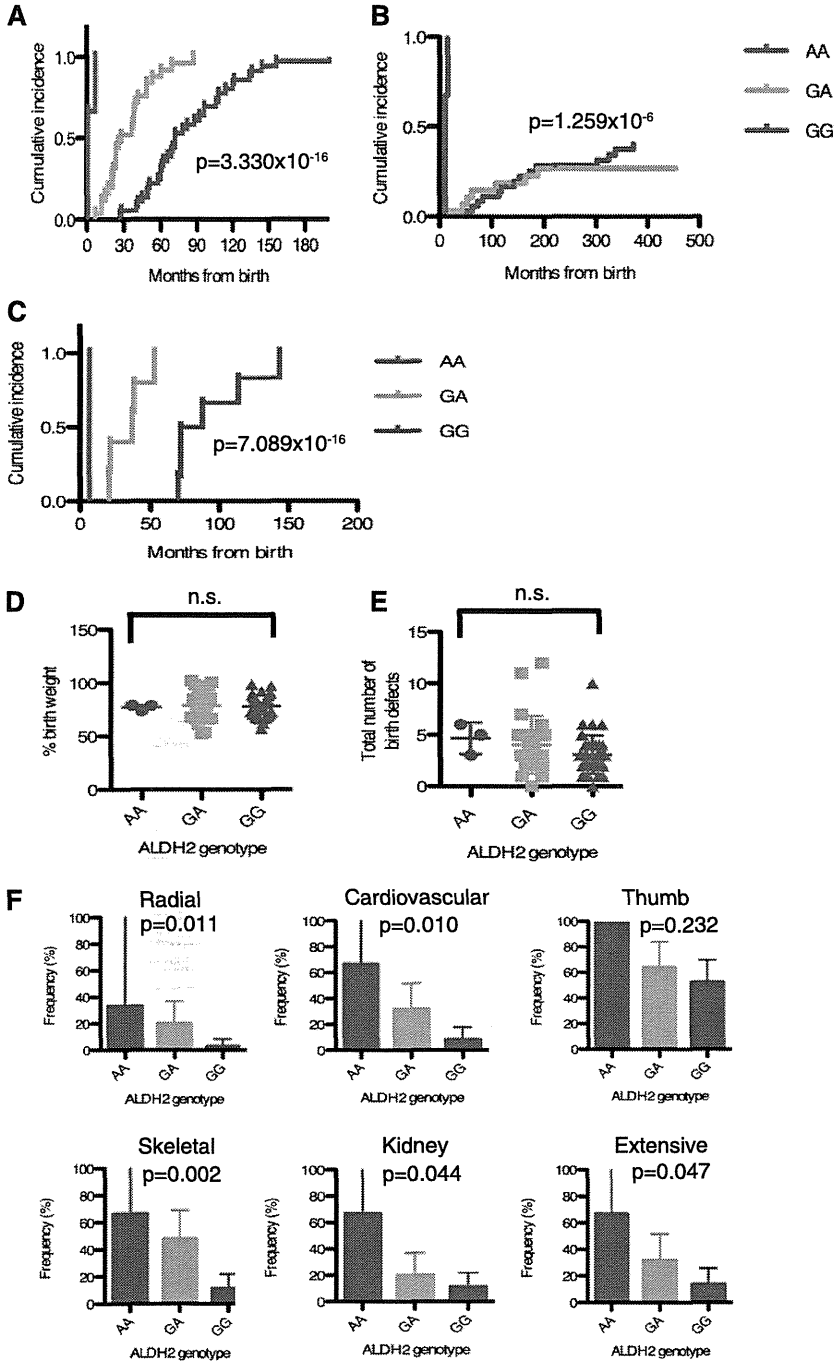

Figure 1. Effects of the ALDH2 deficiency on Japanese FA patients. (A-B) Cumulative incidence of BMF (A) or MDS/AML (B) were analyzed in 64 FA subjects. Numbers of AA, GA, and GG patients were 3, 25, and 36, respectively. (C) Cumulative incidence of BMF was analyzed in patients with confirmed biallelic *FANCA* mutations having protein truncations and/or large deletions (n = 12). Numbers of AA, GA, and GG patients were 1, 5, and 6, respectively. *P* values shown were calculated by the Gray test. In panel A, *P* values between genotypes were 8.625×10^{-7} (GG vs GA), 2.107×10^{-10} (GG vs AA), 1.259×10^{-6} (GA vs AA), respectively. In (B), the difference between GG and GA subjects was not significant ($P = .4564479$), whereas other statistical comparisons were highly significant (GG vs AA, 2.911×10^{-10}; GA vs AA, 8.813×10^{-8}). In panel C, the *P* values between GG and GA, GG and AA, or GA and AA were calculated as 0.001228433, 0.01430588, 0.02534732, respectively. (D) Percentage of birth weight or (E) total number of physical abnormalities (shown in supplemental Table 1) in 64 FA patients with 3 *ALDH2* genotypes. Birth weight was normalized to mean weight at gestational age in Japan. Mean and SEM are indicated. Birth weight records were missing for 3 patients (supplemental Table 1). There was no significant difference between the *ALDH2* genotypes (Kruskal-Wallis test). (F) Frequency (percentage) of cardiovascular, radial, thumb, skeletal, kidney, and extensive malformations in each *ALDH2* genotype. *P* values were calculated by the Cochran-Armitage test for trend, which detects statistical significance of effects across the genotypes. The error bars represent 95% confidence intervals.

Acknowledgments

The authors thank the individual patients and families in the study who made this work possible, Dr K. J. Patel (University of Cambridge) for communicating unpublished results, Dr James Hejna (Graduate School of Biostudies, Kyoto University) for critical reading of the manuscript and English editing, Mr Naoya Suzuki and Drs Akira Niwa and Megumu Saito (CiRA, Kyoto University) for discussion, and Ms Fumiko Tsuchida, Emi Uchida, Sumiyo Ariga, Chinatsu Ohki, and Mao Hisano for expert technical assistance.

This work was supported by grants from the Ministry of Health, Labor and Welfare, and grants from the Ministry of Education, Culture, Sports, Science and Technology (MEXT).

Authorship

Contribution: M.Y. and H.Y. examined DEB-induced chromosome aberrations, carried out MLPA testing, and analyzed clinical records; K.Y., Y.O., Y.S., K.C., H.T., S.M., S.K., and S.O.

performed WES and analyzed sequence data; A.H. validated exome data and carried out genotyping; A.H., M.Y., H.Y., K.M., J.N., and M.T. analyzed data; and M.Y., M.T., and K.M. wrote the paper.

Conflict-of-interest disclosure: The authors declare no competing financial interests.

Correspondence: Minoru Takata, Laboratory of DNA Damage Signaling, Department of Late Effects Studies, Radiation Biology Center, Kyoto University, Kyoto 606-8501, Japan; e-mail: mtakata@house.rbc.kyoto-u.ac.jp; and Miharu Yabe, Department of Cell Transplantation and Regenerative Medicine, Tokai University School of Medicine, Isehara 259-1193, Japan; e-mail: miharu@is.icc.u-tokai.ac.jp.

References

1. Auerbach AD. Fanconi anemia and its diagnosis. *Mutat Res.* 2009;668(1-2):4-10.
2. Kim H, D'Andrea AD. Regulation of DNA cross-link repair by the Fanconi anemia/BRCA pathway. *Genes Dev.* 2012;26(13):1393-1408.
3. Kottemann MC, Smogorzewska A. Fanconi anaemia and the repair of Watson and Crick DNA crosslinks. *Nature.* 2013;493(7432):356-363.
4. Ridpath JR, Nakamura A, Tano K, et al. Cells deficient in the FANC/BRCA pathway are hypersensitive to plasma levels of formaldehyde. *Cancer Res.* 2007;67(23):11117-11122.
5. Langevin F, Crossan GP, Rosado IV, Arends MJ, Patel KJ. Fancd2 counteracts the toxic effects of naturally produced aldehydes in mice. *Nature.* 2011;475(7354):53-58.
6. Garaycoechea JI, Crossan GP, Langevin F, Daly M, Arends MJ, Patel KJ. Genotoxic consequences of endogenous aldehydes on mouse haematopoietic stem cell function. *Nature.* 2012;489(7417):571-575.
7. Parmar K, D'Andrea A, Niedernhofer LJ. Mouse models of Fanconi anemia. *Mutat Res.* 2009; 668(1-2):133-140.
8. Crabb DW, Edenberg HJ, Bosron WF, Li TK. Genotypes for aldehyde dehydrogenase deficiency and alcohol sensitivity. The inactive ALDH2(2) allele is dominant. *J Clin Invest.* 1989; 83(1):314-316.
9. Matsuo K, Hamajima N, Shinoda M, et al. Gene-environment interaction between an aldehyde dehydrogenase-2 (ALDH2) polymorphism and alcohol consumption for the risk of esophageal cancer. *Carcinogenesis.* 2001;22(6):913-916.
10. Butturini A, Gale RP, Verlander PC, Adler-Brecher B, Gillio AP, Auerbach AD. Hematologic abnormalities in Fanconi anemia: an International Fanconi Anemia Registry study. *Blood.* 1994; 84(5):1650-1655.
11. Guardiola P, Pasquini R, Dokal I, et al. Outcome of 69 allogeneic stem cell transplantations for Fanconi anemia using HLA-matched unrelated donors: a study on behalf of the European Group for Blood and Marrow Transplantation. *Blood.* 2000;95(2):422-429.
12. Tachibana A, Kato T, Ejima Y, et al. The FANCA gene in Japanese Fanconi anemia: reports of eight novel mutations and analysis of sequence variability. *Hum Mutat.* 1999;13(3):237-244.
13. Matsuo K, Wakai K, Hirose K, Ito H, Saito T, Tajima K. Alcohol dehydrogenase 2 His47Arg polymorphism influences drinking habit independently of aldehyde dehydrogenase 2 Glu487Lys polymorphism: analysis of 2,299 Japanese subjects. *Cancer Epidemiol Biomarkers Prev.* 2006;15(5):1009-1013.
14. Kunishima S, Okuno Y, Yoshida K, et al. ACTN1 mutations cause congenital macrothrombocytopenia. *Am J Hum Genet.* 2013;92(3):431-438.
15. Gray RJ. A class of K-sample tests for comparing the cumulative incidence of a competing risk. *Ann Stat.* 1988;16(3):1141-1154.
16. Klein JP, Rizzo JD, Zhang MJ, Keiding N. Statistical methods for the analysis and presentation of the results of bone marrow transplants. Part I: unadjusted analysis. *Bone Marrow Transplant.* 2001;28(10):909-915.
17. Auerbach AD, Rogatko A, Schroeder-Kurth TM. International Fanconi Anemia Registry: relation of clinical symptoms to diepoxybutane sensitivity. *Blood.* 1989;73(2):391-396.
18. Chandrasekharappa SC, Lach FP, Kimble DC, et al; NISC Comparative Sequencing Program. Massively parallel sequencing, aCGH, and RNA-Seq technologies provide a comprehensive molecular diagnosis of Fanconi anemia. *Blood.* 2013;121(22):e138-e148.
19. Wagner JE, Tolar J, Levran O, et al. Germline mutations in BRCA2: shared genetic susceptibility to breast cancer, early onset leukemia, and Fanconi anemia. *Blood.* 2004;103(8):3226-3229.
20. Reid S, Schindler D, Hanenberg H, et al. Biallelic mutations in PALB2 cause Fanconi anemia subtype FA-N and predispose to childhood cancer. *Nat Genet.* 2007;39(2):162-164.
21. Kim Y, Lach FP, Desetty R, Hanenberg H, Auerbach AD, Smogorzewska A. Mutations of the SLX4 gene in Fanconi anemia. *Nat Genet.* 2011; 43(2):142-146.
22. Stoepker C, Hain K, Schuster B, et al. SLX4, a coordinator of structure-specific endonucleases, is mutated in a new Fanconi anemia subtype. *Nat Genet.* 2011;43(2):138-141.
23. Schuster B, Knies K, Stoepker C, et al. Whole exome sequencing reveals uncommon mutations in the recently identified Fanconi anemia gene SLX4/FANCP. *Hum Mutat.* 2013;34(1):93-96.
24. Ceccaldi R, Parmar K, Mouly E, et al. Bone marrow failure in Fanconi anemia is triggered by an exacerbated p53/p21 DNA damage response that impairs hematopoietic stem and progenitor cells. *Cell Stem Cell.* 2012;11(1):36-49.
25. Chen CH, Budas GR, Churchill EN, Disatnik MH, Hurley TD, Mochly-Rosen D. Activation of aldehyde dehydrogenase-2 reduces ischemic damage to the heart. *Science.* 2008;321(5895): 1493-1495.

Biosystems. The following primer sequences were used: *GAPDH* forward, 5′-AACAGCCTCAAGATCATCAGC-3′; *GAPDH* reverse, 5′-TTGGCAGGTTTTTCTAGACGG-3′; *MPL* primer 1 forward, 5′-CAGCGAGTCCTCTTTGTGG-3′; *MPL* primer 1 reverse, 5′-CCCAGCTGATCTGAAGTTCC-3′; *MPL* primer 2 forward, 5′-AGGCCATCAGGACTGGAA-3′; *MPL* primer 2 reverse, 5′-CAGCTGTAAACGGTAGCGAGA-3′; *MPL* primer 3 forward, 5′-GGTGACCGCTCTGCATCTA-3′; *MPL* primer 3 reverse, 5′-CAGGGCATGCCTCAGTCT-3′; *KLF1* forward, 5′-ACACCAAGAGCTCCCACCT-3′; *KLF1* reverse, 5′-GTAGTGGCGGGTCAGCTC-3′.

Statistics. All data are presented as mean ± SD. The statistical significance of the observed differences was determined using 1-way ANOVA for multiple comparisons and 2-tailed Student's *t* tests for pairwise comparisons. A *P* value less than 0.05 was considered significant.

Study approval. The human ESC clone Kyoto hESC-3 (KhES-3) was obtained from the Institute for Frontier Medical Sciences of Kyoto University after approval for human ESC use was granted by the Minister of Education, Culture, Sports, Science, and Technology of Japan (MEXT). Dermal fibroblasts derived from a CAMT patient were obtained at University of Saga School of Medicine (Saga, Japan) under informed consent. The Review Boards for ethics at the Institute of Medical Science, The University of Tokyo, and University of Saga School of Medicine approved this research protocol, including the informed consent. The entire study was conducted in accordance with the Declaration of Helsinki.

Acknowledgments

The authors thank N. Nakatsuji, H. Suemori, T. Kitamura, A. Hotta, M. Onodera, T. Yamaguchi, and N. Komatsu for providing reagents and cells. The authors also thank A. Watanabe for performing bisulfite sequence analysis and providing useful suggestions. This work was supported by Project of realization of regenerative medicine (phase II) from MEXT (to K. Eto and H. Nakauchi) and a Grant-in-aid (Kaken) for Young Scientist from MEXT (to N. Takayama). This research was also supported in part by the Japan Society for the Promotion of Science (JSPS) through its "Funding Program for World-Leading Innovative R&D on Science and Technology" (FIRST Program) to N. Takayama, S. Nakamura, and T. Dohda.

Received for publication May 9, 2012, and accepted in revised form May 30, 2013.

Address correspondence to: Koji Eto or Naoya Takayama, Clinical Application Department, Center for iPS Cell Research and Application, Kyoto University, 53 Kawahara-cho, Shogoin, Sakyo-ku, Kyoto 606-8507, Japan. Phone: 81.75.366.7075; Fax: 81.75.366.7095; E-mail: kojieto@cira.kyoto-u.ac.jp (K. Eto), naoya.takayama@cira.kyoto-u.ac.jp (N. Takayama).

1. Yoshihara H, et al. Thrombopoietin/MPL signaling regulates hematopoietic stem cell quiescence and interaction with the osteoblastic niche. *Cell Stem Cell.* 2007;1(6):685–697.
2. Qian H, et al. Critical role of thrombopoietin in maintaining adult quiescent hematopoietic stem cells. *Cell Stem Cell.* 2007;1(6):671–684.
3. de Sauvage FJ, et al. Physiological regulation of early and late stages of megakaryocytopoiesis by thrombopoietin. *J Exp Med.* 1996;183(2):651–656.
4. Alexander WS, Roberts AW, Nicola NA, Li R, Metcalf D. Deficiencies in progenitor cells of multiple hematopoietic lineages and defective megakaryocytopoiesis in mice lacking the thrombopoietic receptor c-Mpl. *Blood.* 1996;87(6):2162–2170.
5. Kaushansky K. The molecular mechanisms that control thrombopoiesis. *J Clin Invest.* 2005;115(12):3339–3347.
6. Drachman JG, Griffin JD, Kaushansky K. The c-Mpl ligand (thrombopoietin) stimulates tyrosine phosphorylation of Jak2, Shc, and c-Mpl. *J Biol Chem.* 1995;270(10):4979–4982.
7. Ihara K, et al. Identification of mutations in the c-mpl gene in congenital amegakaryocytic thrombocytopenia. *Proc Natl Acad Sci U S A.* 1999;96(6):3132–3136.
8. Ballmaier M, et al. c-mpl mutations are the cause of congenital amegakaryocytic thrombocytopenia. *Blood.* 2001;97(1):139–146.
9. King S, Germeshausen M, Strauss G, Welte K, Ballmaier M. Congenital amegakaryocytic thrombocytopenia: a retrospective clinical analysis of 20 patients. *Br J Haematol.* 2005;131(5):636–644.
10. Carver-Moore K, et al. Low levels of erythroid and myeloid progenitors in thrombopoietin-and c-mpl-deficient mice. *Blood.* 1996;88(3):803–808.
11. Takayama N, Eto K. Pluripotent stem cells reveal the developmental biology of human megakaryocytes provide a source of platelets for clinical application. *Cell Mol Life Sci.* 2012;69(20):3419–3428.
12. Park IH, et al. Disease-specific induced pluripotent stem cells. *Cell.* 2008;134(5):877–886.
13. Raya A, et al. Disease-corrected haematopoietic progenitors from Fanconi anaemia induced pluripotent stem cells. *Nature.* 2009;460(7251):53–59.
14. Ye Z, et al. Human-induced pluripotent stem cells from blood cells of healthy donors and patients with acquired blood disorders. *Blood.* 2009;114(27):5473–5480.
15. Zou J, Mali P, Huang X, Dowey SN, Cheng L. Site-specific gene correction of a point mutation in human iPS cells derived from an adult patient with sickle cell disease. *Blood.* 2011;118(17):4599–4608.
16. Zou J, et al. Gene targeting of a disease-related gene in human induced pluripotent stem and embryonic stem cells. *Cell Stem Cell.* 2009;5(1):97–110.
17. Sun N, et al. Patient-specific induced pluripotent stem cells as a model for familial dilated cardiomyopathy. *Sci Transl Med.* 2012;4(130):130ra47.
18. Lu SJ, et al. Biologic properties and enucleation of red blood cells from human embryonic stem cells. *Blood.* 2008;112(12):4475–4484.
19. Kobari L, et al. Human induced pluripotent stem cells can reach complete terminal maturation: in vivo and in vitro evidence in the erythropoietic differentiation model. *Haematologica.* 2012;97(12):1795–1803.
20. Chang CJ, et al. Production of embryonic and fetal-like red blood cells from human induced pluripotent stem cells. *PloS One.* 2011;6(10):e25761.
21. Muraoka K, et al. Successful bone marrow transplantation in a patient with c-mpl-mutated congenital amegakaryocytic thrombocytopenia from a carrier donor. *Pediatr Transplant.* 2005;9(1):101–103.
22. Takayama N, et al. Generation of functional platelets from human embryonic stem cells in vitro via ES-sacs, VEGF-promoted structures that concentrate hematopoietic progenitors. *Blood.* 2008;111(11):5298–5306.
23. Takayama N, et al. Transient activation of c-MYC expression is critical for efficient platelet generation from human induced pluripotent stem cells. *J Exp Med.* 2010;207(13):2817–2830.
24. Takayama N, Eto K. In vitro generation of megakaryocytes and platelets from human embryonic stem cells and induced pluripotent stem cells. *Methods Mol Biol.* 2012;788:205–217.
25. Ory DS, Neugeboren BA, Mulligan RC. A stable human-derived packaging cell line for production of high titer retrovirus/vesicular stomatitis virus G pseudotypes. *Proc Natl Acad Sci U S A.* 1996;93(21):11400–11406.
26. Muraoka K, et al. Defective response to thrombopoietin and impaired expression of c-mpl mRNA of bone marrow cells in congenital amegakaryocytic thrombocytopenia. *Br J Haematol.* 1997;96(2):287–292.
27. Vodyanik MA, Thomson JA, Slukvin II. Leukosialin (CD43) defines hematopoietic progenitors in human embryonic stem cell differentiation cultures. *Blood.* 2006;108(6):2095–2105.
28. Klimchenko O, et al. A common bipotent progenitor generates the erythroid and megakaryocyte lineages in embryonic stem cell-derived primitive hematopoiesis. *Blood.* 2009;114(8):1506–1517.
29. Nishikii H, et al. Metalloproteinase regulation improves in vitro generation of efficacious platelets from mouse embryonic stem cells. *J Exp Med.* 2008;205(8):1917–1927.
30. Kobayashi M, Laver JH, Kato T, Miyazaki H, Ogawa M. Recombinant human thrombopoietin (Mpl ligand) enhances proliferation of erythroid progenitors. *Blood.* 1995;86(7):2494–2499.
31. Parekh C, et al. Novel pathways to erythropoiesis induced by dimerization of intracellular C-Mpl in human hematopoietic progenitors. *Stem Cells.* 2012;30(4):697–708.
32. Lu J, et al. MicroRNA-mediated control of cell fate in megakaryocyte-erythrocyte progenitors. *Dev Cell.* 2008;14(6):843–853.
33. Bouilloux F, et al. EKLF restricts megakaryocytic differentiation at the benefit of erythrocytic differentiation. *Blood.* 2008;112(3):576–584.
34. Dore LC, Crispino JD. Transcription factor networks in erythroid cell and megakaryocyte development. *Blood.* 2011;118(2):231–239.
35. Starck J, et al. Functional cross-antagonism between transcription factors FLI-1 and EKLF. *Mol Cell Biol.* 2003;23(4):1390–1402.
36. Wang Y, Fan PS, Kahaleh B. Association between enhanced type I collagen expression and epigenetic repression of the FLI1 gene in scleroderma fibroblasts. *Arthritis Rheum.* 2006;54(7):2271–2279.
37. Israel MA, et al. Probing sporadic and familial Alzheimer's disease using induced pluripotent stem cells. *Nature.* 2012;482(7384):216–220.
38. Dimos JT, et al. Induced pluripotent stem cells generated from patients with ALS can be differentiated into motor neurons. *Science.* 2008;321(5893):1218–1221.
39. Bilican B, et al. Mutant induced pluripotent stem cell lines recapitulate aspects of TDP-43 proteinopathies and reveal cell-specific vulnerability. *Proc*

In summary, we used CAMT iPSCs to demonstrate that MPL signaling is indispensable for maintenance of MPPs and for transition from MPPs to MEPs during early hematopoiesis. Its absence led to deficiencies in both erythropoiesis and megakaryopoiesis, although some development of myeloid cells was retained (Figure 7). This constellation of effects recapitulates the clinical course seen in CAMT patients. We were also able to show the true pathogenesis of CAMT, whereby lineage commitment by MEPs toward erythropoiesis is the result of a dysregulated program of activated modification of FLI1 gene expression. These findings also provide a rationale for the use of MPL-stimulating drugs (i.e., TPO mimetics) in the treatment of anemia as well as other ailments, such as thrombocytopenia and stem cell suppression.

Methods

Further information can be found in Supplemental Methods.

Cells, reagents, and viral vectors. pMX and pMY retroviral vectors were a gift from T. Kitamura (The University of Tokyo, Tokyo, Japan). pGCDNsam IRES EGFP retroviral vector was from M. Onodera (National Children's Research Center, Tokyo, Japan). The CSII lentiviral vector was from T. Yamaguchi (The University of Tokyo, Tokyo, Japan). pMX mRFP1 retroviral vector was from A. Hotta (CiRA, Kyoto University, Kyoto, Japan). The human ESC line was from N. Nakatsuji and H. Suemori (Institute for Frontier Medical Sciences, Kyoto University, Kyoto, Japan). A normal human iPSC clone, TkDA3-4, was used as a reference (23). The UT-7/TPO cell line was from N. Komatsu (Juntendo University, Tokyo, Japan).

CAMT fibroblasts were cultivated in DMEM supplemented with 10% FBS, 2 mM L-glutamine, 100 U/ml penicillin, and 0.1 mg/ml streptomycin (all from Invitrogen). Disease-specific iPSCs derived from dermal fibroblasts from a CAMT patient (CAMT iPSCs) were established using retroviral vectors harboring 4 reprogramming factors (*OCT3/4*, *SOX2*, *KLF4*, and *c-MYC*; clones 1 and 2) or 3 reprogramming factors (*OCT3/4*, *SOX2*, and *KLF4*; clone 3), as previously described (23). All PSCs were maintained as described previously (23). The mouse C3H10T1/2 cell line was purchased from the RIKEN Bio-Resource Center and was cultured as described previously (23). Retroviral supernatants for establishing iPSCs were obtained from a 293 GPG system (provided by R.C. Mulligan, Children's Hospital Boston, Boston, Massachusetts, USA) (25). Human VEGF, TPO, and SCF were from R&D Systems. Human EPO was from Kyowa Hakko Kirin Co. Heparin was from Ajinomoto Pharmaceuticals Co. The metalloproteinase inhibitor GM-6001 was from Cosmobio Co. The following antibodies were used (from BD, unless indicated otherwise): allophycocyanin- (APC-) or PE/Cy7-conjugated anti-CD34, APC-conjugated anti-CD41a (integrin αIIb; HIP8 clone), eFluor 450–conjugated anti-CD42a (GPIX) (eBioscience), PE-conjugated anti-CD42b (GPIbα), PE-conjugated anti-CD43 (eBioscience), Alexa Fluor 405–conjugated anti–glycophorin A (GPA) (Biolegend), PE-conjugated anti-pAKT, anti-pERK1/2, anti-pSTATA3, and anti-pSTAT5.

Hematopoietic differentiation of human ESCs and iPSCs. Differentiation of human ESCs and iPSCs into hematopoietic cells was performed as described previously (22–24). In brief, small clumps of human PSCs (<100 cells treated with PBS containing 0.25% trypsin (Invitrogen), 1 mM $CaCl_2$ (Sigma-Aldrich), and 20% KSR (Invitrogen) were transferred onto mitomycin-treated or irradiated C3H10T1/2 cells and cocultured in hematopoietic cell differentiation medium, which was replaced every 3 days. On days 14–15 of culture, the HPCs within ESC- and iPSC-Sacs were collected and then sorted into $CD34^+$ HPCs, $CD34^+CD43^+CD41a^-GPA^-$ MPPs, and $CD41a^+GPA^+$ MEPs using an Aria flow cytometer (BD). They were then transferred onto freshly mitomycin-treated or irradiated feeder cells and further cultivated in differentiation medium supplemented with TPO and combinations of other cytokines/mediators/inhibitors (50 ng/ml SCF, 25 U/ml heparin sodium, 6 U/ml EPO, and 50 μM GM-6001), as described previously (22–24, 29). The medium was refreshed every 3 days, and nonadherent cells were collected and analyzed daily from day 16 to day 24.

Retroviral and lentiviral vectors and infection. Full-length *MPL* was subcloned into the retroviral vector pMY IRES EGFP (55). Full-length *FLI1* was subcloned into the retroviral vector pGCDNsam IRES EGFP or lentiviral vector pCSII harboring 2A mRFP1. Viral supernatant was generated as previously described (56). CAMT iPSCs, normal iPSCs, or ESCs were transduced with either vehicle vector or pMY-MPL-EGFP, after which $EGFP^+$ iPSCs were sorted using a flow cytometer. $CD34^+$ HPCs derived from normal iPSCs, with or without MPL overexpression, were also transduced with vehicle, pGCDNsam FLI1-EGFP, or pCS2 FLI1-RFP. This was followed by 8 days of culture in the presence of SCF, TPO, and EPO.

Hematopoietic colony-forming cell assay. Hematopoietic colony-forming cell assays were performed as described previously (23). In brief, $CD34^+$ HPCs from within iPSC-Sacs were cultivated for 14 days in MethoCult H4434 semisolid medium (Stem Cell Technologies Inc.) supplemented with 50 ng/ml human TPO. The colonies were then collected, stained with Hemacolor (Merck), and observed under a microscope.

Flow cytometric analysis of hematopoietic cells. Nonadherent cells on days 16–24 of culture were prepared in PBS containing 3% FBS (staining medium) and stained with combinations of antibodies for 30 minutes on ice. Samples were then washed with staining medium and analyzed by flow cytometry. Dead cells were identified using PI and excluded. Precise numbers of the cells were estimated using True Count Beads (BD Biosciences).

Flow cytometric analysis of polyploidy in MKs. Nonadherent cells on days 22–24 were prepared in staining medium and stained with 25 μg/ml Hoechst 33342 (Sigma-Aldrich) for 45 minutes at 37°C, followed by anti-human CD41a-APC and CD42b-PE for 30 minutes. Samples were then washed with cold staining medium and analyzed by flow cytometry in the presence of PI.

Flow cytometric analysis of platelets. Washed platelets were prepared as described previously (22). The resultant platelet pellets were resuspended with staining medium and stained with anti-human CD41a-APC, CD42a-Pacific blue, and CD42b-PE for 30 minutes at room temperature. The platelets were then diluted in 200 μl staining medium and analyzed by flow cytometry. Platelet numbers were estimated using True Count Beads.

Flow cytometric analysis of the cell cycle. Nonadherent cells from among MPPs on days 14 + 2 of culture were prepared in staining medium and stained with Vybrant DyeCycle Violet Stain (Invitrogen) for 30 minutes at 37°C. Samples were then stained with PI and analyzed by flow cytometry.

Phosphorylation of downstream molecules of MPL. $CD34^+$ HPCs derived from human iPSCs were starved overnight in differentiation medium containing 0.5% FBS, stained with CD34-APC for 30 minutes at 37°C, and then stimulated for 10 minutes with 100 ng/ml TPO. Immediately thereafter, they were fixed with Lyse/Fix buffer (BD) for 10 minutes at 37°C, permeabilized with Perm buffer III (BD) for 30 minutes on ice, and immunostained for pAKT, pERK1/2, pSTAT3, and pSTAT5 using PE-conjugated antibodies at room temperature for 1 hour. Samples were then washed with staining medium and analyzed by flow cytometry. Similarly, MKs in differentiation medium supplemented with SCF, TPO, and heparin on days 22–24 were stained with anti-CD41a-APC for 30 minutes at 37°C. They were then fixed, permeabilized, stained for downstream mediators, and analyzed as the HPCs were.

Quantitative RT-PCR. After sorting $CD34^+$ HPCs using flow cytometry, RNA was extracted and cDNA was synthesized as described previously (22). Real-time PCR was performed using an EagleTaq Master Mix with ROX and Universal Probe Library kit (Roche Applied Science) according to the manufacturer's instructions. Signals were detected using an ABI7900HT Real-Time PCR System (Applied Biosystems). Primer sets for *GAPDH*, *MPL*, and *KLF1* were determined using the Universal Probe Library Set for humans (http://www.roche-applied-science.com/sis/rtpcr/upl/index.jsp?id=UP030000). Primer sets for *FLI1* (Hs00956711_m1) were purchased from Applied

HPCs, and that the effect might be determined primarily by FLI1 expression downstream of TPO/MPL signaling. Another important finding of this study was that complimentary transduction of *MPL* into CAMT iPSCs using a retroviral vector enabled expression of different levels of MPL and revealed the critical importance of MPL-mediated signaling. Taken together, these findings indicate that the strength of the intracellular signaling of TPO/MPL to downstream mediators may determine lineage-dependent fate and behavior and that this important process is completely dysregulated by loss of MPL in CAMT patients.

Patients with CAMT exhibit severe thrombocytopenia, which most often begins at birth and worsens into bone marrow failure with aplastic anemia during childhood or sooner. These features ultimately lead to death unless the patient is successfully treated with HSC transplantation. King et al. provided detailed descriptions of the clinical symptoms and disease courses in 20 CAMT patients (9). These patients were divided into 2 groups, CAMT-I and CAMT-II, based on the time course of the platelet counts during their first year of life, which correlated well with the behavior of the pancytopenia and the type of MPL mutations (9). CAMT-I patients exhibited biallelic nonsense or frameshift mutation of *MPL*, leading to complete null expression of the mRNA. These patients had very low platelet counts and developed severe bone marrow failure during childhood. CAMT-II patients exhibited single amino acid substitutions in the intracellular domain of MPL but retained some residual MPL function, which appeared to delay the onset of bone marrow failure compared with CAMT-I patients. The most critical manifestation in both types of this disease was severe thrombocytopenia and anemia, which were evident prior to leukopenia (9). These findings are consistent with the notion that individual hematopoietic lineages have different dependencies on MPL signaling; however, the precise link between MPL and lineage commitment and blood cell generation at defined differentiation steps remains unclear, in large part because of the difficulty of examining HSCs obtained directly from CAMT patients. The $Mpl^{-/-}$ mouse model, which has normal erythrocyte and leukocyte counts throughout life despite sustained thrombocytopenia, does not recapitulate the human phenotype, illustrating the difference in the MPL signal dependencies of mice and humans. We therefore created human iPSCs using fibroblasts from a CAMT-I patient (7, 21) with compound heterozygous nonsense and frameshift mutations in the *MPL* locus (Supplemental Figure 3). These mutations generated a premature stop codon, leading to rapid degradation of the mutated mRNA through nonsense-mediated mRNA decay (41). In fact, none of the truncated MPL proteins or mRNAs could be detected in $CD34^+$ HPCs derived from CAMT iPSCs (Supplemental Figure 3, A–C).

In vitro hematopoietic differentiation assays to track the progression of blood generation revealed that the $CD34^+CD43^+CD41a^-GPA^-$ MPPs derived from iPSC clones created from healthy human specimens can be differentiated into $CD41a^+GPA^+$ cells, which contain a MEP population (28) able to give rise to a proper balance of $CD41a^+GPA^-$ MKs and $CD41a^-GPA^+$ erythrocytes (Figure 3, B and C). In contrast, maintenance of the MPP population and the transition from MPPs to MEPs were completely blocked in CAMT iPSCs (Figure 3, D–F), although some potential for differentiation into the granulocyte and macrophage lineages was retained (Figure 2D). Unlike MPPs derived from normal iPSCs, those from CAMT iPSCs produced smaller numbers of $CD43^+$ cells (Figure 3G), consistent with the pancytopenia seen in CAMT patients and indicative of the role of human MPL signaling in MPPs. Moreover, administration of a nonpeptide TPO mimetic, eltrombopag, improved pancytopenia in patients with aplastic anemia (42), suggesting the potential importance of MPL signaling in human HSCs/HPCs. This is consistent with our novel finding that MPL was indispensable for normal erythropoiesis. Thus, by using CAMT iPSCs, we were able to recapitulate the clinical course of CAMT patients, including the distinct features of their blood cell generation and maintenance during childhood (9).

It was previously suggested that in order to keep platelet production in the normal range, MPL signaling must fall within a window that is presumably regulated by either definite serum level of TPO (43, 44), level of MPL expression and its subsequent dimerization and internalization (45), or various inhibitory signaling molecules (5). One possible mechanism for the dysregulation of CAMT iPSC–derived HPCs is a deficiency in MPL signaling, which could also account for the childhood thrombocytopenia observed in patients. Interestingly, experiments involving MPL expression in normal and CAMT iPSCs strongly implied that regulation of the transcriptional factor FLI1, downstream of TPO/MPL at the $CD34^+$ HPC level, is impaired in CAMT. For dominant production of erythrocytes (rather than MKs) through normal hematopoiesis in humans, erythrocytes must outnumber platelets 20:1. In that case, erythrocytes would likely outnumber MKs 40,000:1, as platelet/MK generation is estimated to be about 2,000:1 (46). Under the conditions of normal human cells, stronger TPO/MPL signaling may suppress FLI1 activity (Figure 6, B and C); determining the mechanism underlying the aberrant FLI1 expression in CAMT iPSCs will require further study.

Our present study also showed that excessive MPL signaling in both normal and CAMT iPSCs led to deleterious megakaryopoiesis and production of $CD41a^+CD42b^-CD42a^-$ MKs and platelets (Figure 5). Furthermore, we confirmed that these aberrant CD42-null platelets were dysfunctional in terms of inside-out signaling (data not shown). Similar aberrant hematopoiesis with greater numbers of immature MKs and reduced erythropoiesis seen with CAMT iPSCs overexpressing MPL is observed clinically in myeloproliferative disease (MPD) patients carrying the MPLW515 mutant, a constitutively active, TPO-hypersensitive mutant that transduces a signal stronger than that of WT MPL upon TPO stimulation (47–49). The degree of similarity between HPCs from MPLW515 patients and the CAMT iPSCs in this study remains uncertain, but both cells are expected to exhibit hematopoiesis that differs from normal.

MKs derived from both normal and CAMT iPSC–derived HPCs overexpressing MPL in the presence of TPO showed augmented pSTAT3, pSTAT5A, and pAKT, but not pERK. However, we were unable to identify the specific downstream signaling molecule(s) responsible for the aberrant megakaryopoiesis through single transduction of a constitutively active form of AKT (50) or STAT5A (Stat5 1*6) (51, 52) into $CD34^+$ HPCs derived from human ESCs (data not shown). This implies that enhanced signaling by STAT3 and/or other mediators is involved in the blockade of MK maturation and that MPL expression level governs MK maturation.

CAMT patients require HSC transplantation to survive, but a suitable donor is not always available. iPSC technology may enable development of new gene correction/administration therapies using the patients' own HSCs. In that regard, induction of adult-type HSCs from human PSCs was recently accomplished in vivo through teratoma formation in NOD.Cg-*Prkdc*^{scid} *Il2rg*^{tm1Wjl}/SzJ (NSG) and NOD/SCID mice (53, 54).

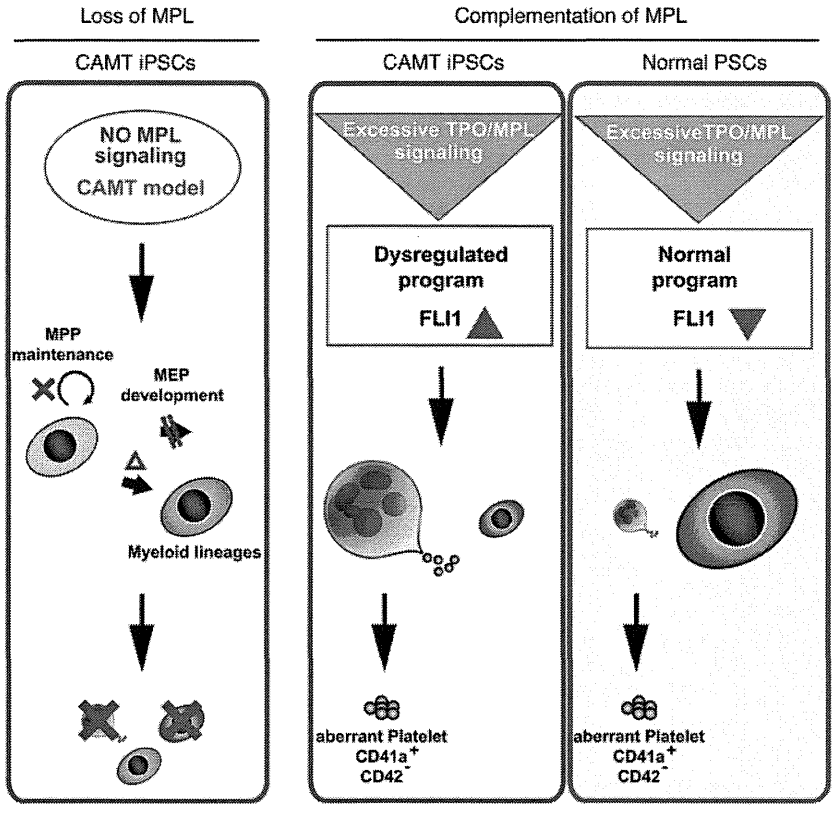

Figure 7
Model of human megakaryopoiesis and erythropoiesis regulated by MPL signaling. CAMT iPSC behavior showed that MPL signaling is essential for MPP maintenance and the development of MEPs from MPPs. In addition, MPL contributes to further myeloid development, but it is not indispensable, which indicates that the dependency on MPL signaling varies among lineages. MPL complementation experiments yielded 2 important findings. First, CAMT iPSCs exhibit dysregulated differentiation toward megakaryopoiesis and erythropoiesis, which is characterized by MK-biased differentiation due to intrinsically dominant FLI1 expression accelerated by ectopic TPO/MPL signaling. Conversely, FLI1 expression is diminished and erythropoiesis is dominant in normal PSCs. Second, excessive TPO/MPL signaling impairs MK maturation and facilitates generation of aberrant CD41a$^+$ and CD42-null platelets from both normal and CAMT iPSCs.

FLI1 were observed with MK-biased differentiation in CAMT iPSC-derived cells (Figure 6B and Supplemental Figure 11A). It is noteworthy that the *FLI1* expression profile at the CD34$^+$ progenitor stage was completely reversed between normal and CAMT iPSC-derived HPCs: *FLI1* expression was reduced in normal iPSC-derived CD34$^+$ HPCs but markedly elevated in CAMT iPSC-derived CD34$^+$ HPCs in a manner dependent on exogenous MPL expression, and this profile persisted even after differentiation (Figure 6, B and C). On the other hand, KLF1 expression behavior appeared to show a similar pattern, but only after differentiation (Supplemental Figure 11, A and B). This suggests that FLI1 is primarily involved in the fate decision from pluripotent stem cell-derived (PSC-derived) MEPs, which may subsequently affect KLF1 function.

We next confirmed that overexpression of FLI1 plus EGFP in CD34$^+$ HPCs derived from normal iPSCs facilitated MK-biased differentiation of the CD34$^+$ HPCs compared with HPCs overexpressing EGFP alone (Figure 6D). More importantly, lentiviral transduction of the same normal CD34$^+$ HPC population overexpressing MPL plus EGFP with red fluorescent protein-labeled (RFP-labeled) FLI1 diminished erythrocyte-biased differentiation (Figure 6E). Furthermore, *FLI1* mRNA levels were well correlated with RFP levels in PSCs, even in the presence of elevated MPL, whereas *KLF1* levels were inversely related to RFP levels (Supplemental Figure 12). These results indicate that CD34$^+$ HPCs derived from CAMT iPSCs exhibit MK-biased differentiation due to impairment of *FLI1* transcriptional factor. Hypermethylation of the *FLI1* promoter reportedly suppresses *FLI1* expression, leading to reduced collagen synthesis in fibroblasts derived from patients with scleroderma fibrosis (36). However, bisulfite sequence analysis of the *FLI1* promoter region revealed that most CpGs in CD34$^+$ HPCs derived from normal and CAMT iPSCs overexpressing MPL were unmethylated and did not significantly differ (data not shown). We therefore conclude that the opposite behavior of CAMT versus normal iPSC-derived HPCs is associated with hyperactivation of *FLI1*, independent of its DNA methylation status.

Discussion

Disease-specific iPSCs are a powerful tool for replacing invaluable cellular resources that are difficult or impossible to obtain from patients, enabling one to recapitulate a disease phenotype in stepwise fashion during differentiation in vitro (11). For example, the difficulty in obtaining living neurons from patients limits understanding of the pathogenesis of degenerative nerve diseases. On the other hand, in vitro neuronal differentiation systems using patient-derived iPSCs have contributed to clarifying the developmental pathogenesis of some diseases (37–40). Similarly, the rarity of MKs within bone marrow is closely associated with our inability to study normal and pathological megakaryopoiesis and platelet generation directly, especially in patients with severely reduced megakaryopoiesis. In that context, we used an in vitro disease tracing system with CAMT iPSCs to make 2 novel findings about the effect of MPL signaling on human hematopoiesis (Figure 7). First, a loss-of-function study revealed the diversity of MPL signaling required among hematopoietic lineages and recapitulated the clinical course of CAMT. Second, a gene complementation (gain-of-function) study using 2 normal iPSC clones and 4 CAMT iPSC clones overexpressing MPL showed that the program governing differentiation toward MKs or erythrocytes was impaired in CAMT iPSC-derived

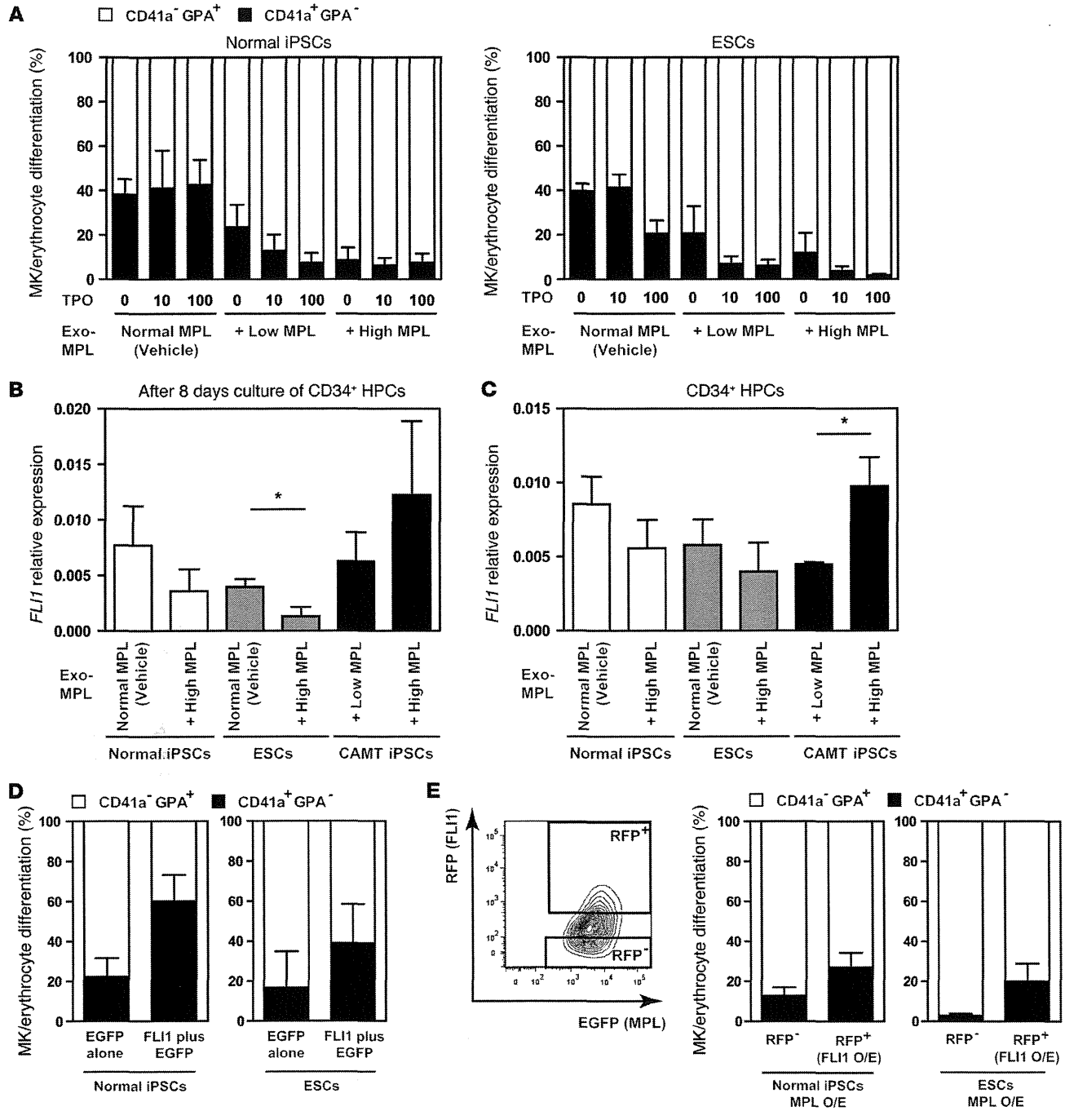

Figure 6

FLI1-mediated MK/erythrocyte differentiation differed between normal and CAMT iPSCs. Shown are results for MK and erythrocyte generation from CD34⁺ HPCs on day 22. (**A**) Percent CD41⁺GPA⁻ MKs and CD41⁻GPA⁺ erythrocytes derived from normal iPSCs (left) or ESCs (right) and transduced with vehicle or MPL expression vector in the presence of 0, 10, or 100 ng/ml TPO with SCF and EPO. Exogenous MPL expression was assessed based on EGFP fluorescence intensity. Erythropoiesis was enhanced in a TPO/MPL signaling–dependent manner. (**B** and **C**) *FLI1* expression in CD34⁺ HPCs before (**C**) and after (**B**) differentiation. EGFP^{hi} CD34⁺ HPCs derived from normal iPSCs and ESCs with or without MPL overexpression, or EGFP^{lo} or EGFP^{hi} CD34⁺ HPCs from CAMT iPSCs overexpressing MPL, were sorted and cultivated for an additional 8 days. (**D**) Percent MK and erythrocyte differentiation from CD34⁺ HPCs derived from normal iPSCs or ESCs overexpressing EGFP alone (vehicle) or FLI1 plus EGFP. (**E**) Percent MK and erythrocyte differentiation from normal iPSCs or ESCs overexpressing MPL-EGFP and FLI1-RFP. CD34⁺ HPCs derived from normal iPSCs or ESCs overexpressing MPL were transfected with FLI1-RFP or vector and cultivated for an additional 8 days. Exogenous FLI1 expression was assessed based on RFP expression (shown in the contour plot). FLI1 overexpression attenuated erythrocyte-biased differentiation in normal iPSCs and ESCs. $^*P < 0.05$.

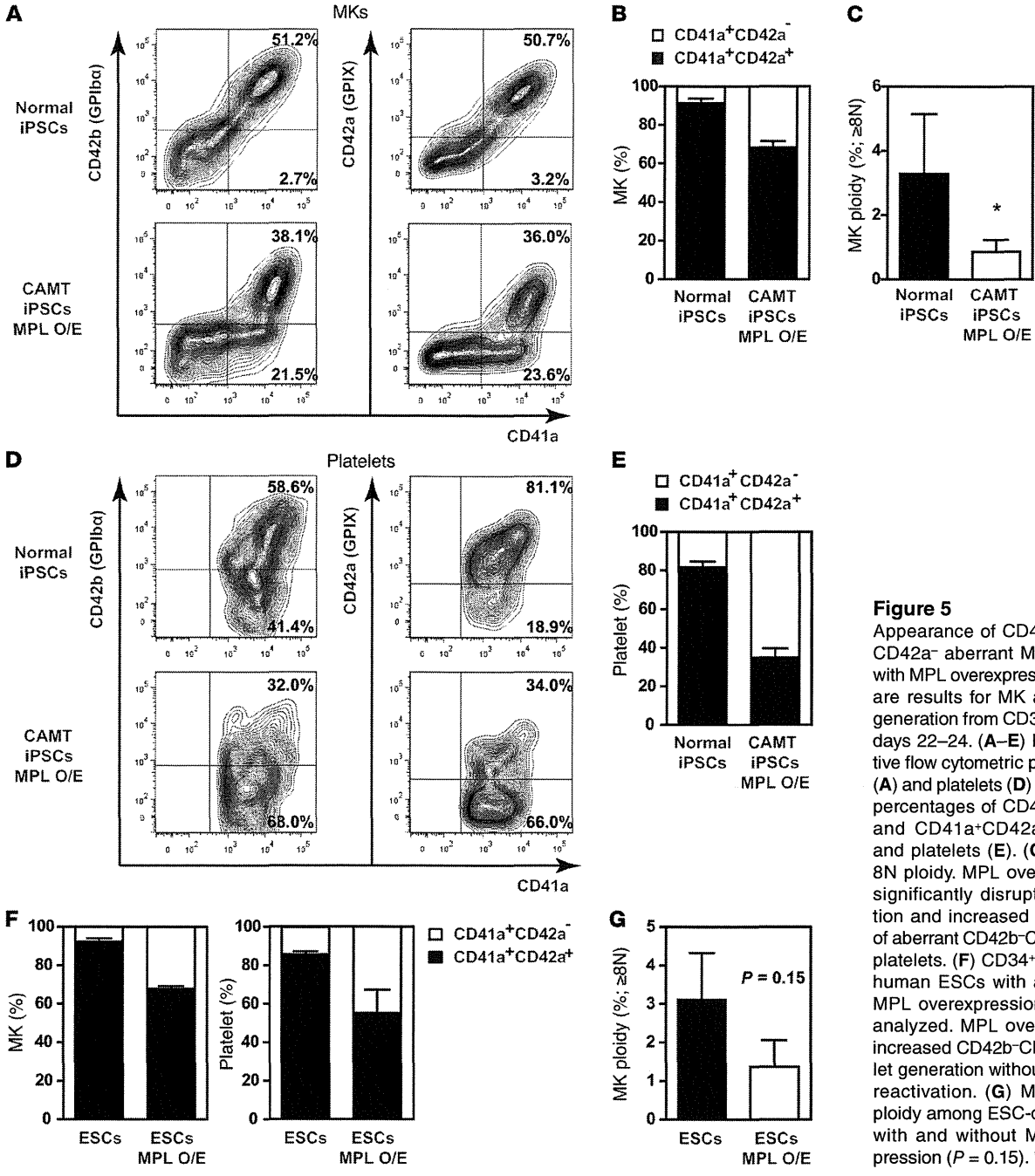

Figure 5

Appearance of CD41a+CD42b-CD42a- aberrant MKs/platelets with MPL overexpression. Shown are results for MK and platelet generation from CD34+ HPCs on days 22–24. (**A**–**E**) Representative flow cytometric plots for MKs (**A**) and platelets (**D**) and the final percentages of CD41a+CD42a- and CD41a+CD42a+ MKs (**B**) and platelets (**E**). (**C**) MKs with 8N ploidy. MPL overexpression significantly disrupted maturation and increased populations of aberrant CD42b-CD42a- MKs/platelets. (**F**) CD34+ HPCs from human ESCs with and without MPL overexpression were also analyzed. MPL overexpression increased CD42b-CD42a- platelet generation without transgene reactivation. (**G**) MKs with 8N ploidy among ESC-derived MKs with and without MPL overexpression ($P = 0.15$). *$P < 0.05$.

of normal iPSC- or ESC-derived CD34+ HPCs into MKs or erythrocytes in the presence of SCF, TPO, and EPO was manipulated by varying the level of exogenous MPL expression. Consistent with an earlier report (31), normal CD34+ HPCs strongly expressing MPL showed erythrocyte-biased differentiation that was dependent on TPO/MPL signaling (Figure 6A and Supplemental Figure 10). This suggests that the program of differentiation toward MKs or erythrocytes distinctly differs between normal and CAMT iPSC-derived CD34+ HPCs and that the lineage balance in normal iPSC-derived HPCs may correspond to normal erythropoiesis in vivo and in vitro (28, 32, 33). Although the underlying mechanism governing lineage commitment toward MKs or erythrocytes is not fully understood, it appears that Friend leukemia virus integration 1 (FLI1) and Kruppel-like factor 1 (KLF1) are potential fate-determining transcriptional factors at the MEP stage and that they mutually antagonize one another (34, 35). Therefore, to evaluate the fate determination program in normal and CAMT iPSC-derived CD34+ HPCs, we used quantitative PCR to assess *FLI1* and *KLF1* expression. Consistent with the mutually antagonistic relationship between FLI1 and KLF1 as well as with earlier reports (28, 34), higher *KLF1* and lower *FLI1* expression were observed with erythrocyte-biased differentiation in normal iPSC-derived cells, whereas lower *KLF1* and higher

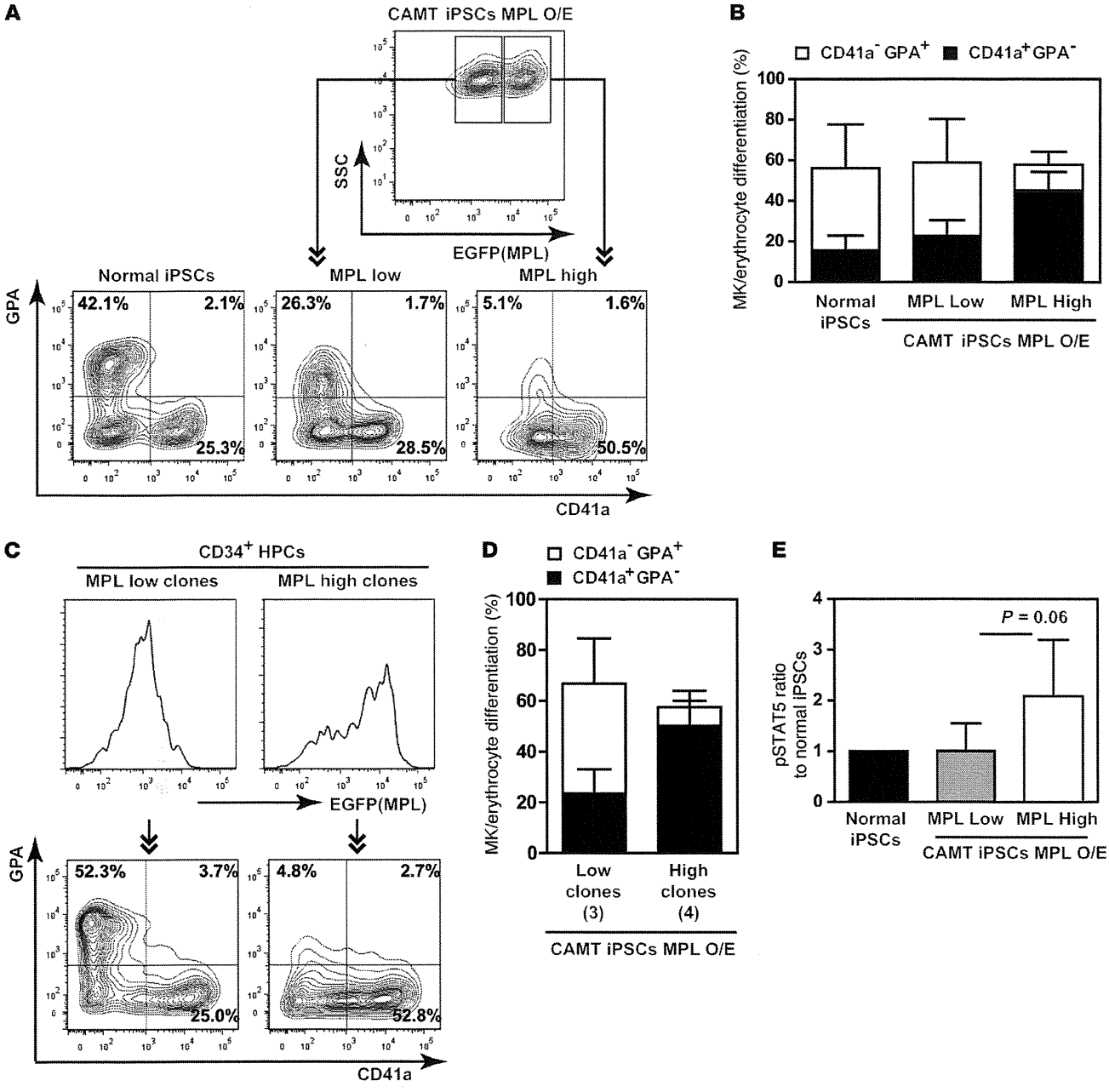

Figure 4

MPL expression levels may determine MK and erythrocyte specification. (**A**) Representative flow cytometric plots of MK and erythrocyte differentiation on day 22. EGFP^{hi} and EGFP^{lo} populations of CAMT iPSCs overexpressing MPL were retrospectively reanalyzed for CD41a and GPA expression. (**B**) Percent CD41a$^-$GPA$^+$ erythrocytes and CD41a$^+$GPA$^-$ MKs from the indicated iPSCs. High MPL expression led to preferential differentiation into MKs. (**C**) EGFP^{hi} and EGFP^{lo} CD34$^+$ HPC populations derived from several CAMT iPSC clones with MPL overexpression are shown as histograms and flow cytometric plots. Representative plots after induction of differentiation are shown for each clone (high and low MPL intensity). (**D**) Percent MK/erythrocyte differentiation. The number of clones is indicated in parentheses. MPL expression level affected the MK/erythrocyte lineage commitment of CD34$^+$ HPCs. (**E**) CD34$^+$ HPCs were incubated with TPO and analyzed for pSTAT5. Results are presented as fluorescence intensity relative to that of normal iPSCs (assigned as 1). The population with higher MPL overexpression showed a markedly augmented TPO-mediated response ($P = 0.06$).

Loss of MPL signaling in CAMT iPSCs impairs FLI1-mediated lineage determination toward erythrocytes or MKs. As shown in Figure 4, the strong intensity of TPO/MPL signaling influenced dominant differentiation into MKs from CAMT iPSC–derived CD34$^+$ HPCs at the expense of erythropoiesis. However, in normal hematopoiesis, some reports showed that TPO/MPL signaling contributed to erythropoiesis (30, 31). To assess the relationship between MPL signal intensity and erythropoiesis in normal cells, the differentiation

Retroviral complementation of WT MPL restored hematopoiesis to CAMT iPSCs. To determine whether complementation of WT MPL in CAMT iPSCs could restore blood generation, CAMT iPSCs were transduced with *MPL* and *EGFP* using retroviral vectors and then purified by sorting out EGFP$^+$ cells using the differentiation protocol depicted in Figure 2A. CAMT iPSCs transduced with vehicle vector showed severely impaired generation of MKs, platelets, and erythrocytes, although they retained reduced granulocyte and macrophage differentiation potential in colony formation assays (Figure 2, B–D). Conversely, overexpression of MPL in CAMT iPSCs restored the differentiation potential of all myeloid cell lineages to levels comparable to those seen in normal iPSCs (Figure 2, B–D).

TPO/MPL signaling was indispensable for MPP maintenance and transition to common MEPs. Earlier studies demonstrated that, in an in vitro hematopoietic differentiation system using human ES cells (ESCs), CD34$^+$CD43$^+$CD41a$^-$GPA$^-$ and CD41a$^+$GPA$^+$ populations represent multipotent hematopoietic progenitors (MPPs) (27) and MEPs (28), respectively (Figure 3A). We evaluated whether human iPSCs exhibit traceable differentiation steps, similar to those seen with normal dermal fibroblast–derived iPSCs, in our differentiation system. CD34$^+$CD43$^+$CD41a$^-$GPA$^-$ MPPs sorted on day 14 of culture differentiated into CD41a$^+$GPA$^+$ MEPs on additional day +4, which in turn differentiated into CD41a$^+$GPA$^-$ MKs (25.7%) and CD41a$^-$GPA$^+$ erythrocytes (40.6%) on additional day +8 (Figure 3B). We then further confirmed that the selected CD41a$^+$GPA$^+$ MEPs could be differentiated into both CD41a$^+$GPA$^-$ MKs (20.0%) and CD41a$^-$GPA$^+$ erythrocytes (66%) on additional day +8 (Figure 3C). In our culture system, therefore, CD34$^+$CD43$^+$CD41a$^-$GPA$^-$ MPPs derived from normal iPSCs had the potential to generate CD41a$^+$GPA$^+$ MEPs that preferentially differentiated into erythrocytes rather than MKs (Figure 3, B and C).

CAMT iPSCs transduced with vehicle vector showed severely defective transition from MPPs to MEPs, which was corrected in CAMT iPSCs overexpressing MPL (Figure 3, D and E). In addition, whereas the number of MPPs derived from normal or CAMT iPSCs overexpressing MPL was maintained at least until day 4, the number of cells derived from untreated CAMT iPSCs declined rapidly, even in the presence of SCF and TPO (Figure 3F). Consequently, fewer CD43$^+$ pure hematopoietic cells were derived from CAMT iPSCs (Figure 3G). In addition, serial replating assays revealed that CD34$^+$ HPCs derived from CAMT iPSCs generated a few colonies exclusively in the first replating trial, whereas CD34$^+$ HPCs from normal iPSCs or from ESCs produced much larger numbers of colonies, even after the second replating trial (Supplemental Figure 4), which implies impairment of self-replication by CAMT iPSC–derived MPPs. The smaller numbers of MPPs could potentially be accounted for by increased apoptosis (sub-G1 population) and/or decreased proliferation (S/G2/M populations) (Figure 3H and Supplemental Figure 5); however, this was more likely due to the loss of MPL. Collectively, these results indicate that MPL signaling is essential for the transition of MPPs to MEPs as well as for MPP maintenance, and that MPL also contributes to their differentiation into granulocytes and macrophages (Figure 2D). Notably, this differentiation profile was consistent with the clinical course in CAMT patients, who typically show early onset of severe thrombocytopenia and anemia prior to leukopenia (9) and HSC exhaustion.

Supplementing CD34$^+$ HPCs derived from CAMT iPSCs with normal levels of MPL contributed to lineage commitments to both MKs and erythrocytes, but higher levels blocked erythropoiesis. Retroviral gene transduction is a powerful tool for studying the actions by a gene of interest. We noted that the expression levels obtained after MPL supplementation in CAMT iPSCs paralleled fluorescence intensity after retroviral transduction–mediated EGFP expression (Supplemental Figure 6, A and B). On day 22 of culture, normal iPSC–derived MPPs could be differentiated into both erythrocytes and MKs in the presence of SCF, TPO, and EPO. Under these conditions, they preferentially differentiated into erythrocytes (Figure 4, A and B). Flow cytometric analysis showed that a CAMT iPSC clone overexpressing MPL produced 2 distinct populations exhibiting different levels of EGFP expression (EGFP^{hi} and EGFP^{lo}; indicative of high and low MPL expression, respectively) on day 22 of culture (Figure 4A). The EGFP^{lo} population showed nearly equal levels of erythrocyte and MK differentiation, similar to normal iPSCs. However, the EGFP^{hi} population showed apparently increased MK differentiation, with few erythrocytes (Figure 4, A and B). These results were identical to results obtained in a prospective analysis in which CD34$^+$ HPCs derived from 7 individual CAMT iPSC clones were EGFP^{hi} or EGFP^{lo} on day 14, faithfully reflecting MPL expression level — i.e., EGFP^{hi} and EGFP^{lo} populations equalized at 10 times normal and at normal levels of MPL, respectively (Supplemental Figure 6), and were respectively subjected to the differentiation protocol (Figure 4, C and D). We also confirmed that the intensity of EGFP expression, as detected by flow cytometry, corresponded well to the level of pSTAT5 (Figure 4E). Based on our results thus far, we concluded that the intensity of MPL signaling determines the fate of erythrocyte and MK differentiation at the MPP stage and that excessive MPL signaling may block erythrocyte differentiation in CAMT iPSCs.

Excessive TPO/MPL signaling in MKs induces aberrant megakaryopoiesis, leading to generation of CD42b$^-$ platelets. As shown in Figure 2B, 3 times as many MKs were generated from CAMT iPSCs overexpressing MPL than from normal iPSCs. The level of *MPL* expression in CD34$^+$ HPCs derived from CAMT iPSCs overexpressing MPL was greater than in those from normal iPSCs (Supplemental Figure 6B); however, the numbers of CD42b$^+$ platelets were similar, which suggests that excessive MPL signaling might adversely influence megakaryopoiesis. Flow cytometric analysis on day 24 of culture revealed that CAMT iPSCs overexpressing MPL generated greater numbers of MKs showing incomplete maturation — i.e., with both CD41a$^+$CD42b$^-$CD42a$^-$ and CD41a$^+$CD42b$^-$CD42a$^+$ populations and low ploidy (Figure 5, A–C). Moreover, the dysregulated MKs appeared to release CD41a$^+$CD42b$^-$CD42a$^-$ platelets (Figure 5, D and E), even in the presence of GM-6001 (Supplemental Figure 7), which we previously showed to induce retention of CD42b on platelets by preventing its metalloproteinase-catalyzed shedding (29).

We also previously showed that excessive c-MYC activation in MKs blocks MK maturation and leads to CD42b^{lo} platelet generation (23). We therefore tested whether overexpression of MPL in human ESCs also blocks MK maturation in association with reduced platelet generation. Indeed, ESCs overexpressing MPL did generate the immature type of CD41a$^+$CD42b$^-$CD42a$^-$ MKs with lower ploidy and CD41a$^+$CD42b$^-$CD42a$^-$ platelets (Figure 5, F and G). We therefore concluded that excessive MPL signaling induces dysregulation of thrombopoiesis, which might be related to the MPL signaling level, as evidenced by the increased TPO sensitivity of CAMT iPSCs overexpressing MPL (Supplemental Figure 8). In addition, flow cytometric analysis suggested that the augmented MPL signaling might be associated with increased pAKT, pSTAT3, or pSTAT5A, but not pERK1/2, in CD41a$^+$ MKs (Supplemental Figure 9), which indicates that excessive signaling impairs normal MK development.

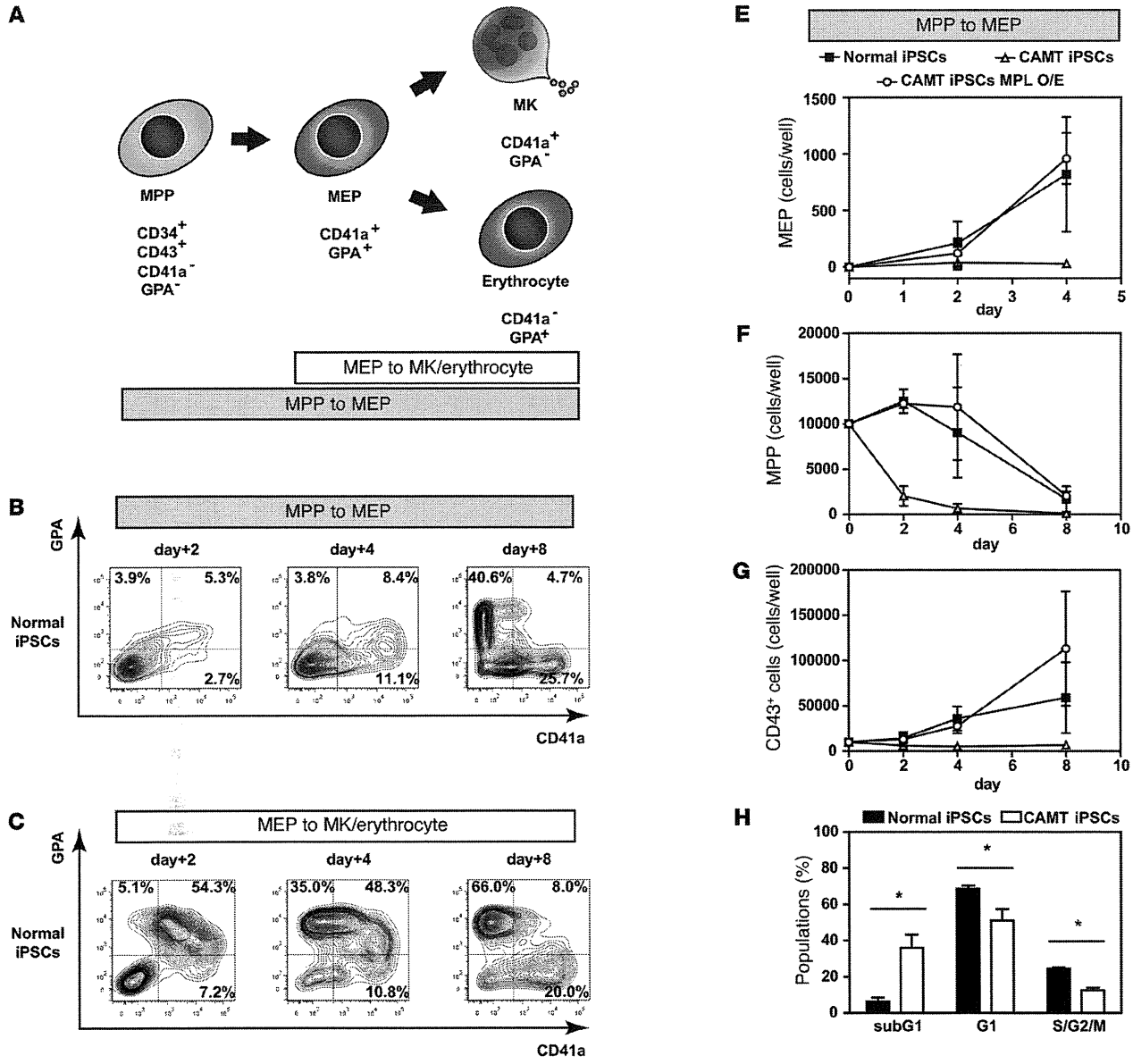

Figure 3

Essential role for MPL signaling in MPP maintenance and MEP development. (**A**) Putative in vitro differentiation from CD34+CD43+CD41a− GPA− MPPs into CD41a+GPA+ MEPs, and subsequently into MKs/erythrocytes. MPPs or MEPs were cultured with SCF, TPO, and EPO for 2–8 days. (**B–D**) Representative flow cytometric plots for MPPs derived from normal (**B**) or CAMT (**D**) iPSCs, and for MEPs derived from normal iPSCs (**C**). (**E**) Numbers of MEPs (cells/well) were plotted to illustrate the kinetics of MEP development from MPPs. MPL expression was required for MEP development. (**F**) Time-dependent loss of MPPs derived from normal and CAMT iPSCs, with or without MPL overexpression, in the presence of SCF, TPO, and EPO. Reduction kinetics were calculated as the absolute number of MPPs. The data indicated the critical role of MPL expression in MPPs. (**G**) Kinetics of CD43+ hematopoietic cell generation from the MPPs in **F**. (**H**) Percentage of individual cell cycle phases in the MPPs in **F** on day 2 of culture. Increase in sub-G1 (reflecting apoptosis) and decrease in S/G2/M (reflecting proliferation) were observed in MPPs derived from CAMT iPSCs. These results suggest that MPL deficiency has a significant effect on apoptosis among progenitors. *$P < 0.05$.

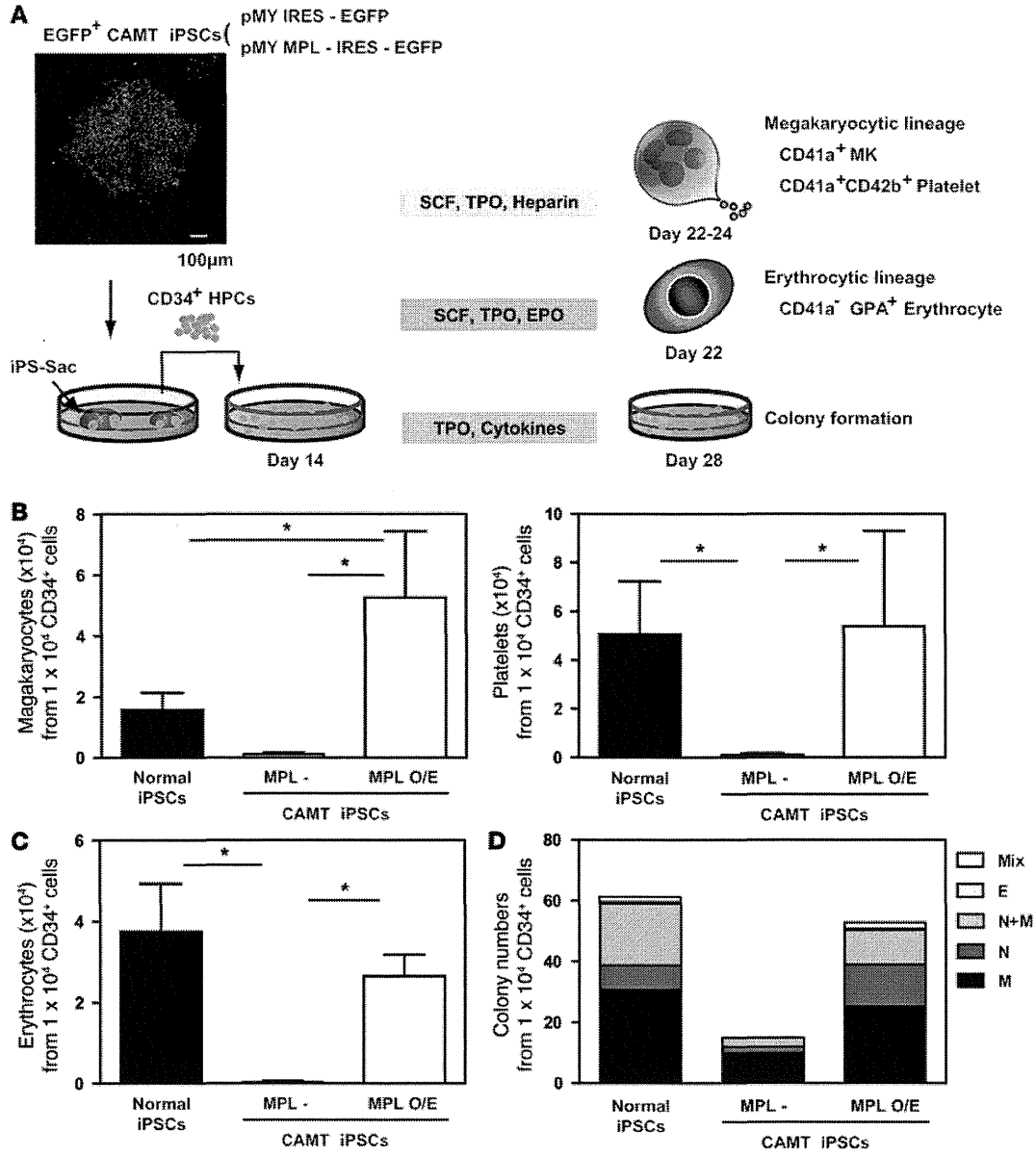

Figure 2

Disease phenotype of CAMT iPSCs was seemingly restored by MPL supplementation. (**A**) In vitro differentiation protocol using CAMT iPSCs transduced with *MPL*. CAMT iPSCs were transduced using a pMY retroviral vector harboring *EGFP* and *MPL* or *EGFP* alone and then selected as EGFP+ populations. Using the indicated cytokines, CAMT iPSC–derived EGFP+ CD34+ HPCs overexpressing MPL were subjected to in vitro differentiation toward the MK or erythrocyte lineage or colony formation. Scale bar: 100 μm. (**B** and **C**) Numbers of MKs and platelets (**B**) cultured in SCF, TPO, and heparin for 8–10 days and erythrocytes (**C**) cultured with SCF (50 ng/ml), TPO (10 ng/ml), and EPO (6 U/ml) for 8 days. Cells were cultured without or with supplemental MPL to induce overexpression (O/E). (**D**) Colony-forming potential for myeloid lineage in normal iPSC–derived CD34+ HPCs, and CAMT iPSC–derived EGFP+ CD34+ HPCs with or without MPL supplementation, in MethoCult H4434 semisolid medium containing TPO (50 ng/ml), SCF, EPO, IL-3, and GM-CSF. M, macrophage; N, neutrophil; N+M, neutrophil and macrophage; E, erythrocyte. *$P < 0.05$.

0.56% ± 0.21%; Figure 1B). However, when we reduced the TPO concentration to a more physiological level (0.1–1 ng/ml) (8), platelet numbers from CAMT iPSCs reached 5%–10% of those obtained with normal iPSCs (Supplemental Figure 2); i.e., they approximated the relative numbers obtained in vivo. This finding suggested that CAMT iPSCs recapitulate the thrombocytopenia seen in the CAMT patient, yielding a useful CAMT disease model.

These results were further confirmed by the failure of TPO stimulation to induce phosphorylation of mediators downstream of MPL (i.e., pAKT, pERK1/2, pSTAT3, and pSTAT5) in CD34+ HPCs (Figure 1C) and by the absence of *MPL* mRNA and MPL protein expression (Supplemental Figure 3, A–C), which corresponded to the complete absence of *MPL* expression in bone marrow cells from the patient (26).

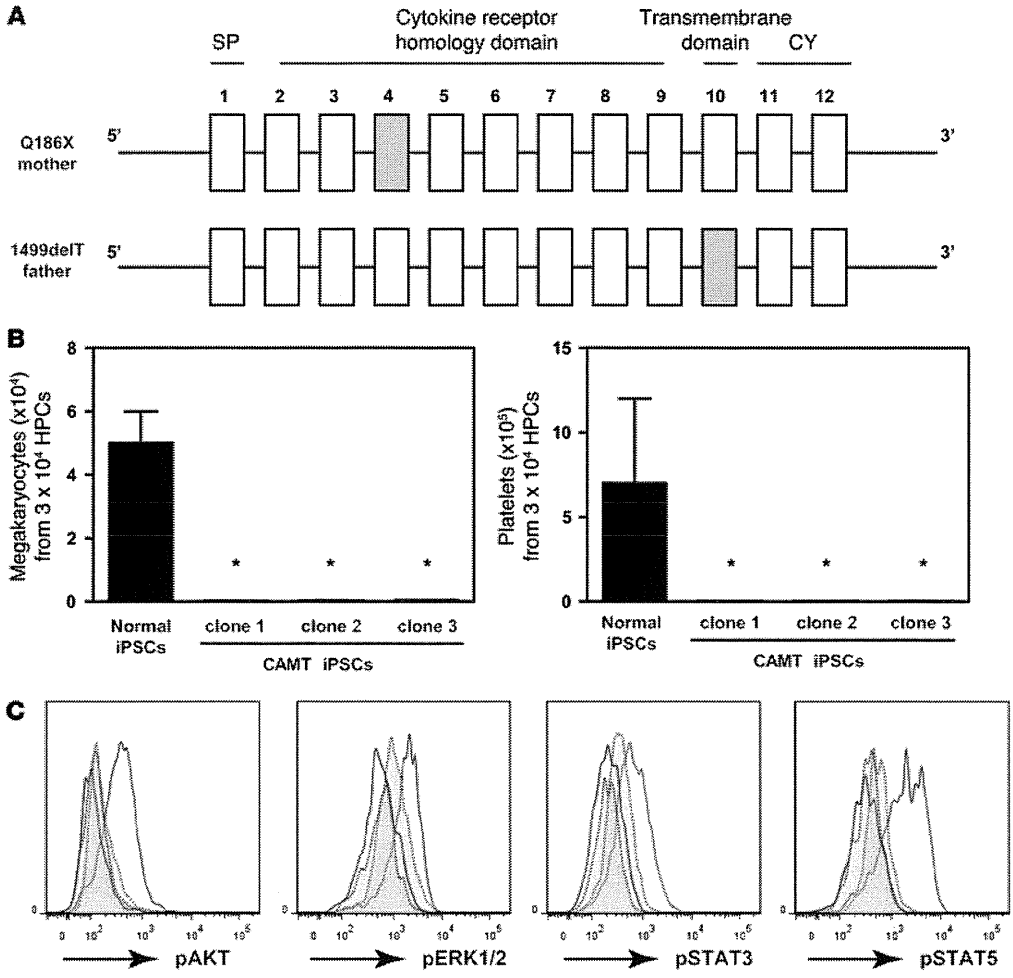

Figure 1

Disease-specific iPSCs recapitulate the disease phenotype manifested in a patient with CAMT. (**A**) Maternal mutation Q186X (C-to-T transition at the cDNA nucleotide position 556) in exon 4 and paternal mutation 1,499delT (single nucleotide deletion of thymine at position 1,499) in exon 10 in a patient with CAMT. SP, signal peptide; CY, cytoplasmic domain. (**B**) Generation of MKs and platelets from normal or CAMT iPSC–derived HPCs cultured on C3H10T1/2 feeder cells for 10 days in the presence of SCF (50 ng/ml), TPO (100 ng/ml), and heparin (25 U/ml). All CAMT iPSC clones generated few MKs or platelets. (**C**) Flow cytometric analysis of MPL-mediated downstream signaling in normal iPSC– (red lines) or CAMT iPSC–derived (blue lines) CD34⁺ HPCs stimulated with 100 ng/ml TPO for 10 minutes (solid lines) or with vehicle control (dotted lines). No response was observed with CAMT iPSCs. *$P < 0.05$.

CAMT. We used skin fibroblasts from the patient to create iPSCs with normal karyotypes using the previously established method with G glycoprotein of the vesicular stomatitis virus (VSV-G) pseudotyped retroviruses (23, 25) harboring 4 (*OCT3/4*, *SOX2*, *KLF4*, and *c-MYC*) or 3 (*OCT3/4*, *SOX2*, and *KLF4*) reprogramming factors (Supplemental Figure 1A; supplemental material available online with this article; doi:10.1172/JCI64721DS1). The resultant CAMT iPSCs exhibited mutations corresponding to the original donor skin, including compound heterozygous point mutations in the *MPL* locus: a C-to-T transition at the cDNA nucleotide position 556 in exon 4, and a single nucleotide deletion of thymine at position 1,499 in exon 10 (Figure 1A and ref. 7). The following parameters were taken as evidence of the pluripotency of CAMT iPSCs: alkaline phosphatase staining; immunostaining for SSEA-4, TRA1-60, and TRA1-81 (Supplemental Figure 1B); gene expression (data not shown); and the capacity for teratoma formation in NOD/SCID mice (Supplemental Figure 1C). We also confirmed that the exogenous reprogramming factors were all silenced in the established iPSCs (data not shown).

To explore the hematopoietic differentiation potential of CAMT iPSCs, we evaluated 3 CAMT iPSC clones and compared them with normal iPSCs (clone TkDA3-4; see Methods) previously established from age-matched dermal fibroblasts using 4 reprogramming factors (23). Using our recently established in vitro differentiation system (22–24), we confirmed that all of the CAMT iPSC clones generated few MKs or platelets, even in the presence of 100 ng/ml TPO, 50 ng/ml stem cell factor (SCF), and 25 U/ml heparin (Figure 1B).

CAMT patients are indeed thrombocytopenic at diagnosis: their platelet counts range 20,000–50,000 platelets/mm^3, equivalent to 5%–10% of that in healthy individuals. Conversely, platelet numbers from CAMT iPSCs in this study were less than 1% of that obtained with normal iPSCs (0.51% ± 0.29%, 0.62% ± 0.42%, and

Research article

Congenital amegakaryocytic thrombocytopenia iPS cells exhibit defective MPL-mediated signaling

Shinji Hirata,[1] Naoya Takayama,[1] Ryoko Jono-Ohnishi,[1] Hiroshi Endo,[1,2] Sou Nakamura,[1] Takeaki Dohda,[1] Masanori Nishi,[3] Yuhei Hamazaki,[3] Ei-ichi Ishii,[4] Shin Kaneko,[1,2] Makoto Otsu,[2] Hiromitsu Nakauchi,[2] Shinji Kunishima,[5] and Koji Eto[1,2]

[1]Clinical Application Department, Center for iPS Cell Research and Application, Kyoto University, Kyoto, Japan. [2]Laboratory of Stem Cell Therapy, Center for Stem Cell Biology and Regenerative Medicine, The Institute of Medical Science, The University of Tokyo, Tokyo, Japan. [3]Department of Pediatrics, University of Saga School of Medicine, Saga, Japan. [4]Department of Pediatrics, University of Ehime School of Medicine, Tohno, Japan. [5]Department of Advanced Diagnosis, Clinical Research Center, National Hospital Organization Nagoya Medical Center, Nagoya, Japan.

Congenital amegakaryocytic thrombocytopenia (CAMT) is caused by the loss of thrombopoietin receptor–mediated (MPL-mediated) signaling, which causes severe pancytopenia leading to bone marrow failure with onset of thrombocytopenia and anemia prior to leukopenia. Because *Mpl*$^{-/-}$ mice do not exhibit the human disease phenotype, we used an in vitro disease tracing system with induced pluripotent stem cells (iPSCs) derived from a CAMT patient (CAMT iPSCs) and normal iPSCs to investigate the role of MPL signaling in hematopoiesis. We found that MPL signaling is essential for maintenance of the CD34$^+$ multipotent hematopoietic progenitor (MPP) population and development of the CD41$^+$GPA$^+$ megakaryocyte-erythrocyte progenitor (MEP) population, and its role in the fate decision leading differentiation toward megakaryopoiesis or erythropoiesis differs considerably between normal and CAMT cells. Surprisingly, complimentary transduction of *MPL* into normal or CAMT iPSCs using a retroviral vector showed that MPL overexpression promoted erythropoiesis in normal CD34$^+$ hematopoietic progenitor cells (HPCs), but impaired erythropoiesis and increased aberrant megakaryocyte production in CAMT iPSC–derived CD34$^+$ HPCs, reflecting a difference in the expression of the transcription factor *FLI1*. These results demonstrate that impaired transcriptional regulation of the MPL signaling that normally governs megakaryopoiesis and erythropoiesis underlies CAMT.

Introduction

It has been well documented that thrombopoietin (TPO) plays an essential role in the self-renewal of HSCs (1, 2) and in the production of megakaryocytes (MKs) and platelets (3, 4). TPO acts via defined signaling pathways that include JAK-STAT, MAPK-ERK1/2, and PI3K-v-akt murine thymoma viral oncogene homolog 1 (PI3K-AKT) (5, 6). Congenital amegakaryocytic thrombocytopenia (CAMT) is a genetic disorder caused by the loss of function or deletion of myeloproliferative leukemia virus oncogene (*MPL*), the gene encoding the TPO receptor (7, 8). CAMT presents at birth with severe thrombocytopenia and absent bone marrow MKs and develops into bone marrow failure/aplastic anemia during the childhood years or even earlier. The disease is fatal unless successfully treated with HSC transplantation, which indicates that TPO/MPL signaling is indispensable for hematopoietic homeostasis in humans. Notably, most CAMT patients show a reduction in platelet and erythrocyte counts prior to the decrease in leukocyte counts (9), and repetitive transfusion of erythrocyte and/or platelets is usually necessary prior to curative bone marrow transplantation. These clinical features imply that each hematopoietic lineage has its own distinct dependency on MPL signaling. On the other hand, the precise roles of MPL at defined differentiation steps during normal hematopoiesis and the effects of its loss in CAMT patients remain unclear, in large part because of the difficulty of obtaining patients' HSCs for in vitro analysis. Although mouse *Tpo*$^{-/-}$ or *Mpl*$^{-/-}$ models show sustained thrombocytopenia with smaller numbers of MKs and smaller myeloid and erythrocyte progenitor pools in the bone marrow (4, 10), they do not fully recapitulate the phenotype manifested in CAMT patients. For example, *Mpl*$^{-/-}$ mice have normal levels of erythrocytes and leukocytes in their peripheral blood throughout life, and live to an old age without developing bone marrow failure/aplastic anemia.

Disease-specific human induced pluripotent stem cells (iPSCs) are an attractive tool for elucidating the pathogenesis of hematological diseases (11–15), for validating gene therapy models (13, 15–17), and for drug screening. Of importance in the present study is that MKs and erythrocytes generated in vitro from disease-specific iPSCs are an effective tool for studying the mechanism of not only thrombopoiesis (11), but also erythropoiesis (18–20).

Here, we established iPSCs derived from a patient diagnosed with CAMT and treated with curative allogenic stem cell transplantation (referred to herein as CAMT iPSCs) (7, 21). In several established CAMT iPSCs, the *MPL* mutations responsible for the complete loss of MPL expression were carried over. Using CAMT iPSCs and an in vitro disease tracking system we established previously (22–24), we determined the precise link between MPL signaling and development of a common MK/erythrocyte progenitor (MEP) and elucidated the pathogenesis of CAMT by recapitulating the clinical manifestations of the disease.

Results

Disease-specific iPSCs from a CAMT patient failed to generate MKs and platelets. A candidate patient was treated with bone marrow transplantation at 12 years of age (7, 21) after being diagnosed with

Conflict of interest: The authors have declared that no conflict of interest exists.

Citation for this article: *J Clin Invest.* 2013;123(9):3802–3814. doi:10.1172/JCI64721.

mTOR pathway, and thereby cause pRb to be phosphorylated,[19] cell-cycle progression in response to the mTOR pathway may be potentiated by the enfeebled function of LxCxE motif of GATA1-S. Thus, we are one step closer to a molecular understanding of GATA1-related leukemias.

Acknowledgments

This work was supported in part by grants-in-aid for scientific research from the Ministry of Education, Culture, Sports, Science and Technology of Japan (R.S., T.T., M.Y., and E.I.), sciences research grants from the Ministry of Health, Labour and Welfare of Japan (E.I.), the Asahi Glass Foundation (R.S.), the Mitsubishi Foundation (R.S. and M.Y.) and the Takeda Foundation (M.Y.).

Authorship

Contribution: T.T., R.K., E.K., H. Kaneko, R.W., and K.T. contributed to the experiments; T.T., M.S., R.S., M.Y., and E.I. contributed to the study design, funding, project conception, and manuscript writing; and H. Kanegane, M.M., M.E., T.M., S.A., and Y.H. contributed to the clinical sample collection and phenotype analyses.

Conflict-of-interest disclosure: The authors declare no competing financial interests.

Correspondence: Masayuki Yamamoto, Department of Medical Biochemistry, Tohoku University Graduate School of Medicine, 2-1 Seiryo-cho, Aoba-ku, Sendai 980-8575, Japan; e-mail: masiyamamoto@med.tohoku.ac.jp; and Etsuro Ito, Department of Pediatrics, Hirosaki University Graduate School of Medicine, 5 Zaifu-cho, Hirosaki, 036-8562, Japan; e-mail: eturou@cc.hirosaki-u.ac.jp.

References

1. Zipursky A, Poon A, Doyle J. Leukemia in Down syndrome: a review. *Pediatr Hematol Oncol.* 1992;9(2):139-149.
2. Hasle H, Niemeyer CM, Chessells JM, Baumann I, Bennett JM, Kerndrup G, Head DR. A pediatric approach to the WHO classification of myelodysplastic and myeloproliferative diseases. *Leukemia.* 2003;17(2):277-282.
3. Hitzler JK. Acute megakaryoblastic leukemia in Down syndrome. *Pediatr Blood Cancer.* 2007;49 (7 Suppl):1066-1069.
4. Malinge S, Izraeli S, Crispino JD. Insights into the manifestations, outcomes, and mechanisms of leukemogenesis in Down syndrome. *Blood.* 2009; 113(12):2619-2628.
5. Wechsler J, Greene M, McDevitt MA, Anastasi J, Karp JE, Le Beau MM, Crispino JD. Acquired mutations in GATA1 in the megakaryoblastic leukemia of Down syndrome. *Nat Genet.* 2002; 32(1):148-152.
6. Xu G, Nagano M, Kanezaki R, et al. Frequent mutations in the GATA-1 gene in the transient myeloproliferative disorder of Down syndrome. *Blood.* 2003;102(8):2960-2968.
7. Rainis L, Bercovich D, Strehl S, et al. Mutations in exon 2 of GATA1 are early events in megakaryocytic malignancies associated with trisomy 21. *Blood.* 2003;102(3):981-986.
8. Harigae H, Xu G, Sugawara T, Ishikawa I, Toki T, Ito E. The GATA1 mutation in an adult patient with acute megakaryoblastic leukemia not accompanying Down syndrome. *Blood.* 2004; 103(8):3242-3243.
9. Hama A, Yagasaki H, Takahashi Y, et al. Acute megakaryoblastic leukaemia (AMKL) in children: a comparison of AMKL with and without Down syndrome. *Br J Haematol.* 2008;140(5):552-561.
10. Muntean AG, Crispino JD. Differential requirements for the activation domain and FOG-interaction surface of GATA-1 in megakaryocyte gene expression and development. *Blood.* 2005; 106(4):1223-1231.
11. Shimizu R, Kobayashi E, Engel JD, Yamamoto M. Induction of hyperproliferative fetal megakaryopoiesis by an N-terminally truncated GATA1 mutant. *Genes Cells.* 2009;14(9): 1119-1131.
12. Li Z, Godinho FJ, Klusmann JH, Garriga-Canut M, Yu C, Orkin SH. Developmental stage-selective effect of somatically mutated leukemogenic transcription factor GATA1. *Nat Genet.* 2005; 37(6):613-619.
13. Kanezaki R, Toki T, Terui K, et al. Down syndrome and GATA1 mutations in transient abnormal myeloproliferative disorder: mutation classes correlate with progression to myeloid leukemia. *Blood.* 2010;116(22):4631-4638.
14. Shapiro MB, Senapathy P. RNA splice junctions of different classes of eukaryotes: sequence statistics and functional implications in gene expression. *Nucleic Acids Res.* 1987;15(17): 7155-7174.
15. Shivdasani RA, Fujiwara Y, McDevitt MA, Orkin SH. A lineage-selective knockout establishes the critical role of transcription factor GATA-1 in megakaryocyte growth and platelet development. *EMBO J.* 1997;16(13):3965-3973.
16. Toki T, Kanezaki R, Adachi S, et al. The key role of stem cell factor/KIT signaling in the proliferation of blast cells from Down syndrome-related leukemia. *Leukemia.* 2009;23(1):95-103.
17. Kadri Z, Shimizu R, Ohneda O, et al. Direct binding of pRb/E2F-2 to GATA-1 regulates maturation and terminal cell division during erythropoiesis. *PLoS Biol.* 2009;7(6):e1000123.
18. Klusmann JH, Godinho FJ, Heitmann K, et al. Developmental stage-specific interplay of GATA1 and IGF signaling in fetal megakaryopoiesis and leukemogenesis. *Genes Dev.* 2010;24(15): 1659-1672.
19. Gera JF, Mellinghoff IK, Shi Y, et al. AKT activity determines sensitivity to mammalian target of rapamycin (mTOR) inhibitors by regulating cyclin D1 and c-myc expression. *J Biol Chem.* 2004; 279(4):2737-2746.

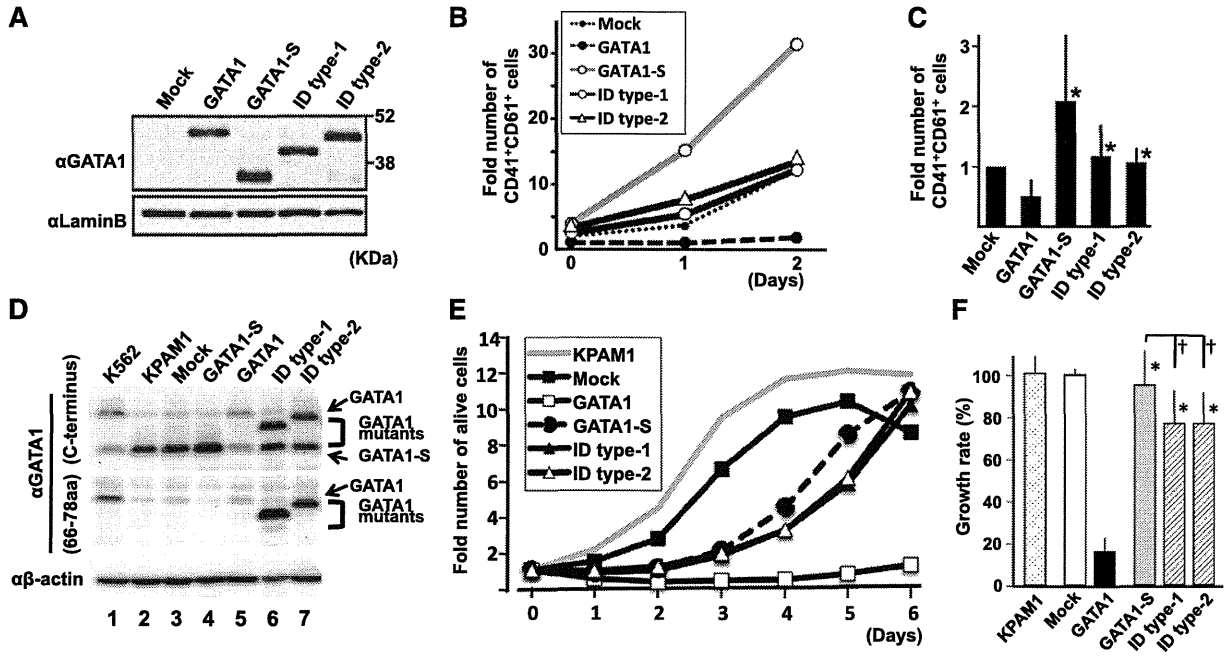

Figure 2. GATA1 ID proteins showed restricted antiproliferative activity. (A) Expression of GATA1 and GATA1 mutant proteins in cultured megakaryocytes at day 0, using an antibody against the C terminus of GATA1. The amount of protein loaded was quantified using an anti-Lamin B antibody on the same membrane. (B) Time-course change in the number of $CD41^+CD61^+$ cells. The value in the mock case at day 0 is set to 1. The result is representative of 4 independent experiments. (C) Comparison of the number of $CD41^+CD61^+$ cells at day 2. The value in the mock case is set to 1 in every experiment. The mean values and standard deviations from 4 independent experiments are presented. Asterisks indicate a significant difference compared with wild-type GATA1 ($P < .05$). (D) Immunoblot analysis of ectopic expression of GATA1 proteins in KPAM1 cells using anti-GATA1 antibodies against C terminus (upper) and residues between amino acids 66 and 78 (middle). The loading volume was quantified using anti-β-actin antibody (lower). (E) Growth curves of KPAM1 cells after ectopic expression of GATA1 proteins. Average values obtained from 6 wells are shown. The value at day zero is set to 1 for each. The growth curve of the original KPAM1 cells was analyzed as a control. Representative data from 3 independent experiments are shown. (F) Relative growth rate of KPAM1 cells at 5 days after ectopic expression of GATA1 mutant proteins. The average value of growth rate in the mock case is set to 100% in every experiment. The mean values and standard deviations from 18 wells obtained in 3 independent experiments (6 wells in each) are presented. Asterisks and daggers indicate significant differences compared with wild-type GATA1 and GATA-S, respectively ($P < .01$).

mutation in GATA1-ID type 2, using alternative acceptor sites in exon 3.

To examine whether the GATA1-ID proteins were produced from the mutant alleles, we performed immunoblotting analysis with 2 distinct antibodies recognizing the C terminus and amino acids 66-78, respectively. We detected GATA1-ID type 1 protein in addition to GATA1-S in the cells transfected with the minigenes harboring Ins 2-bp, Del 2-bp, or Del 7-bp T>A mutations, whereas only GATA1-ID type 2 protein was expressed on transfection of the minigene with a Del 21-bp mutation (Figure 1C). Consistent with the minigene results, a significant amount of GATA1-ID type 1 protein and GATA1-S had accumulated in patients 80 and 37, whereas only GATA1-S was detected in the TAM blasts of patient 86, who had only a short transcript skipping exon 2 because of a point mutation in the exon 2–intron 2 boundary (Figure 1D). Thus, splicing errors were occurred in GATA1-ID type 1 and type 2 patients, leading to the production of GATA1-ID proteins.

We next examined how GATA1-ID proteins affect the proliferation of embryonic megakaryocytic progenitors. We retrovirally transduced GATA1-S and GATA1-ID mutants into lineage-negative cells derived from megakaryocyte-specific *Gata1*-deficient ($Gata1^{\Delta neo\Delta HS}$) embryos[15] and induced differentiation toward the megakaryocytic lineage. The number of $CD41^+CD61^+$ megakaryocytes was significantly higher in cases transduced with GATA1-ID proteins than with wild-type GATA1, despite almost equivalent expression levels of GATA1 proteins (Figure 2A-C). GATA1-S-transduced cells unexpectedly acquired a hyperproliferative potential compared with mock cells, probably because of an unknown function that resides in the GATA1 *N*-terminal region (Figure 2B-C).

We next analyzed cell proliferation using the DS-AMKL cell line KPAM1, in which GATA1-S was predominantly expressed with a very low level of full-length GATA1 (Figure 2D).[16] On transduction with full-length GATA1 retrovirus, proliferation of KPAM1 cells was markedly reduced. In contrast, GATA1-ID type 1 and type 2 moderately restricted the proliferation of KPAM1 cells, but the restriction activity was significantly stronger than that of GATA1-S (Figure 2E-F). These results thus demonstrate that the ID regions indeed contribute to the regulation of AMKL cell proliferation.

Our newly identified GATA1-ID mutants have highlighted a much narrower set of sequences responsible for the pathogenesis of TAM than has previously been suggested by the loss of the *N*-terminal sequence, as in GATA1-S. The missing region identified by the GATA1-ID proteins contains a consensus motif (LxCxE, amino acids 81-85) essential for the interaction with pRb,[17] which is also lost in GATA1-S. Interaction with hypophosphorylated pRb-E2F complex has been reported to be important for GATA1 to support the normal proliferation and differentiation of erythroid progenitors.[17] Consistent with this notion, GATA1-S failed to repress E2F activation, which was followed by activation of mTOR signaling in the GATA1-S fetal megakaryocytes and DS-AMKL cells.[18] Because the protein levels of cyclin D1 and $p27^{Kip}$ are reciprocally regulated by the

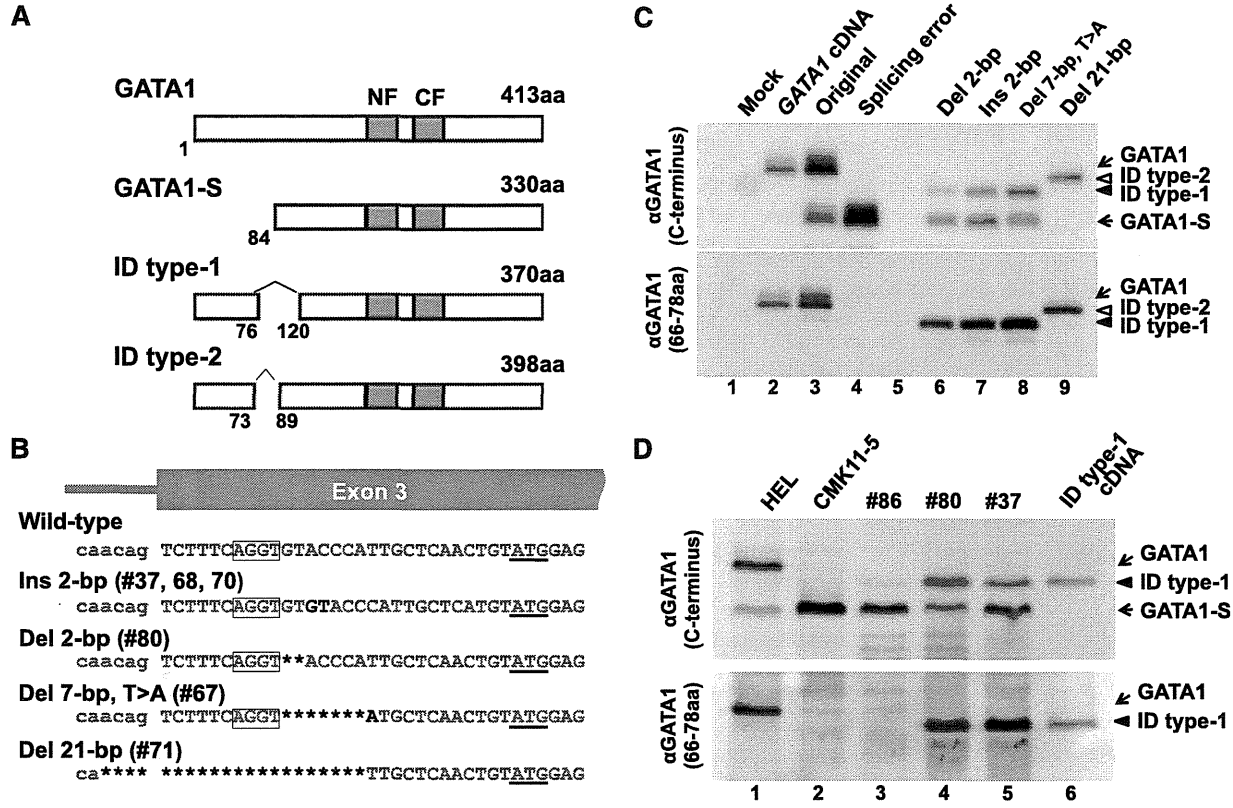

Figure 1. GATA1 mutant proteins with internal deletions. (A) A schema of mutant GATA1 proteins observed in patients with TAM. The amino acid sequence of GATA1-ID proteins was deduced from the sequence of *GATA1* cDNA obtained from patients with TAM. Dark boxes indicate *N*-finger (NF) and C-finger (CF) domains. ID indicates internal deletion. (B) Somatic mutations of the *GATA1* gene found in ID type 1 and type 2 patients. Missing, inserted, or substituted nucleotides are highlighted with dark color. A second translation initiation codon located in the third exon is underlined. The AGGT sequence functioning as an alternative splice donor site in mutant *GATA1* genes of ID type 1 patients is circled. Note that a mutant *GATA1* gene found in TAM patient 71f (ID type 2) lost a splice acceptor site in exon 3 because of the 21-nucleotide deletion. (C) Expression of GATA1 proteins in cells transfected with minigenes using anti-GATA1 antibodies recognizing the C terminus (upper) and residues between the 66th and 78th amino acids (lower) of the GATA1 protein. GATA1-ID proteins are recognized by the antibody against amino acid residues 66-78 of GATA1, whereas GATA1-S is not (lanes 6-9). Cells transfected with mock pcDNA3.1 (lane 1), pcDNA3.1-*GATA1* cDNA (lane 2), original minigene (lane 3), and *GATA1* minigene harboring a splicing error mutant in the 3′ boundary of intron 1[13] (lane 4) are used as positive and negative controls for GATA1 and GATA1-S, respectively. (D) GATA1 ID type 1 protein and GATA1-S are detected in the TAM blast cells from patients 80 (lane 4) and 37 (lane 5), whereas only GATA1-S is expressed in the blast cells from patient 86 harboring a conventional type of *GATA1* gene mutation in TAM cases (lane 3). Note that relatively abundant GATA1-S is recognized in patient 37 because of the intermixing of genetically distinct clone of cells expressing only GATA1-S (supplemental Table 1). Human erythroleukemia cells (HEL, lane 1) were used as a control for GATA1 and GATA1-S. DS-AMKL cells (CMK11-5, lane 2) and BHK-21 cells transfected with cDNA encoding GATA1 ID type 1 protein (lane 6) were used as controls for GATA1-S and GATA1 ID type 1, respectively.

were approved by the Institutional Animal Experiment Committee of Tohoku University. All clinical samples were obtained with informed consent from the parents of all patients with TAM in accordance with the Declaration of Helsinki. Additional information can be found in the supplemental text on the *Blood* website.

Results and discussion

Between 2003 and 2010, we screened *GATA1* mutations by direct sequencing, using cDNAs prepared from TAM blasts provided by 106 patients with DS on request from referring hospitals. Acquired *GATA1* mutations were detected in 99 (93.4%) patients (supplemental Table 1). The majority of the mutations resulted in the GATA1-S mutant protein, which lacks the entire *N*-terminal transactivation domain. Importantly, we found new mutations harboring IDs of 43 and 15 amino acids in 5 patients (patients 37, 67, 68, 70, and 80) and in 1 patient (patient 71), respectively. We refer to these mutants as GATA1-ID type 1 and GATA1-ID type 2, respectively (Figure 1A). Clinical features in patients with TAM who have GATA1-ID mutations were shown in supplemental Table 2. All of these patients showed high white blood cell counts in the peripheral blood, which is known to be a risk factor for early death.[13]

We determined the genomic DNA sequences of these cases. As shown in Figure 1B, the mutations in GATA1-ID type 1 were located in a site immediately 3′ of the consensus motif for a splice donor site AGGT[14] (Ins 2-bp in patients 37, 68, and 70; Del 2-bp in patient 80; and Del 7-bp T>A in patient 67), whereas 21 bp containing a splice acceptor site in front of exon 3 was deleted in GATA1-ID type 2 (Del 21-bp). To verify the transcripts achieved through the putative splice donor site created by mutations in GATA1-ID type 1, we introduced identified mutations into *GATA1* minigene expression vectors[13] and transduced them into hamster fibroblast cell line BHK-21. We found 3 variant transcripts in the cases of GATA1-ID type 1 mutations (supplementary Figure 1A-B): a full-length transcript with deletion or insertion of nucleotides [Ex-2 (+) (PTC)], a short transcript lacking exon 2 by alternative splice variant skipping of exon 2 for GATA1-S [Ex-2 (−)], and an aberrant transcript in which 129 nucleotides were spliced out from exon 3 (Del 129-bp). In contrast, 2 disparate transcripts with deletions of 45 or 137 nucleotides were created by